63-2-3

AD_____

AF 61 (052) – 339

TR

September 1962

TECHNION RESEARCH & DEVELOPMENT

FOUNDATION, HAIFA, ISRAEL



TECHNICAL REPORT

# BUCKLING OF CONICAL SHELLS UNDER EXTERNAL PRESSURE, TORSION AND AXIAL COMPRESSION

Josef Singer

Abraham Eckstein

Menahem Baruch

TECHNION – ISRAEL INSTITUTE OF TECHNOLOGY

DEPARTMENT OF AERONAUTICAL ENGINEERING

HAIFA, ISRAEL.

TAE REPORT 19

AD .....

AF 61 (052) - 339

TR

September 1962

TECHNICAL REPORT

# BUCKLING OF CONICAL SHELLS UNDER EXTERNAL PRESSURE, TORSION AND AXIAL COMPRESSION

Josef Singer,
Abraham Eckstein,
Menahem Baruch
Technion – Israel Institute of Technology
Department of Aeronautical Engineering
Haifa, Israel.

TAE REPORT 19

The research reported in this document has been sponsored by the DIRECTORATE OF AEROSPACE SCIENCES, AFOSR, through the European Office, Aerospace Research United States Air Force.

## FOREWORD

This report covers the second phase of the work carried out under Contract AF 61(052)–339. The first phase was reported in the following Technical Notes and Publications:–

TN 1 (AFOSR TN 60–711), November 1960, "Buckling of Circular Conical Shells Under Axisymmetric External Pressure" (Published in Journal of Mechanical Engineering Science, Vol. 3, No. 4, December 1961).

TN 2 (AFOSR TN 60–860), December 1960, "The Effect of Axial Constraint on the Instability of Thin Conical Shells under External Pressure" (Published in Journal of Applied Mechanics, Vol. 29, No. 1, March 1962).

TN 3 July 1961, "Buckling of Thin Circular Conical Shells Subjected to Axisymmetrical Temperature Distributions and External Pressure".

TN 4 September 1961, "The Effect of Axial Constraint on the Instability of Thin Circular Cylindrical Shells under Uniform Axial Compression" (Published in International Journal of Mechanical Sciences, Vol. 4, No. 2, 1962).

TN 5 December 1961, "A Donnell type Theory for Bending and Buckling of Orthotropic Conical Shells".

"Experimental Investigations of the Instability of Conical Shells under External Pressure", Bulletin of the Research Council of Israel, Vol. 11C, No. 1, April 1962.

# TABLE OF CONTENTS


| | | Page |
|---|---|---|
| | FOREWORD | I |
| | SUMMARY | II |
| | LIST OF FIGURES | III-IV |
| | SYMBOLS | V-VIII |
| SECTION 1. | BUCKLING OF CIRCULAR CONICAL SHELLS UNDER COMBINED TORSION AND EXTERNAL OR INTERNAL PRESSURE<br>by J. Singer and M. Baruch | 1 |
| SECTION 2. | EXPERIMENTAL INVESTIGATION OF THE BUCKLING OF CONICAL SHELLS UNDER UNIFORM HYDROSTATIC PRESSURE<br>by J. Singer and A. Eckstein | 21 |
| SECTION 3. | EXPERIMENTAL INVESTIGATION OF THE BUCKLING OF CONICAL SHELLS UNDER COMBINED TORSION AND EXTERNAL PRESSURE<br>by J. Singer | 34 |
| SECTION 4. | BUCKLING OF CIRCULAR CONICAL SHELLS UNDER UNIFORM AXIAL COMPRESSION<br>by J. Singer | 41 |
| | REFERENCES | 46 |
| | ACKNOWLEDGMENT | 51 |
| | APPENDIX A | 52 |

## S U M M A R Y

A method developed previously for the analysis of the instability of thin conical shells under external pressure is now extended to buckling under torsion and combined torsion and external or internal pressure as well as axisymmetric temperature distributions. The method is based on solution of modified Donnell type stability equations, in the presence of slightly relaxed boundary conditions for the u and v displacements. Two formulations of the solution for torsion and combined loadings are given and compared. Typical examples are calculated and compared with results obtained by Seide, and interaction curves for combined torsion and external pressure loading are given. For conical shells of small and medium taper ratio, the interaction curves may be approximated by the semi-empirical curve of Crate, Batdorf and Baab for cylindrical shells, but for large taper ratio different curves are obtained.

The results of a continuation of an experimental program on the instability of thin truncated conical shells under uniform external pressure, carried out at the Department of Aeronautical Engineering, are presented and discussed. The tests of 33 steel, Alclad, and aluminum alloy conical shells of varying geometries are described, and the results are compared and correlated with other experimental investigations and with theory. The test results reverify the theories of Singer and of Seide. The buckling and postbuckling behaviour and the effect of initial out-of-roundness are discussed.

The results of another experimental program on the instability of thin truncated conical shells in torsion and under the combined loading of external pressure and torsion are given, and compared with the theories of Section 1. Good agreement was obtained between theory and experiments.

The method of analysis of Section 1 is adapted to analyse the asymmetric buckling of thin conical shells under uniform axial compression. A linear theory is used and typical cases are computed and compared with an axisymmetric analysis.

## LIST OF FIGURES


Fig. 1 – Notation

Fig. 2 – Dimensions of Typical Conical Shells Considered in the Analysis

Fig. 3 – Interaction Curves for Truncated Conical Shells Under Combined Torsion and External Hydrostatic Pressure.

Fig. 4 – Test Setup for Combined Torsion and External Pressure Loading.

Fig. 5 – Test Setup – Schematic

Fig. 6 – Device for Measurement of Out-of-Roundness.

Fig. 7 – Typical Initial Circularity Contour (The out-of-roundness is magnified 20 times) – Specimen 421/5

Fig. 8 – Typical Initial Circularity Contour (The out-of-roundness is magnified 20 times) – Specimen 321/4

Fig. 9 – Typical Specimens – Steel

Fig. 10 – Typical Specimens – Alclad

Fig. 11 – Typical Buckle Pattern in Fully Buckled State, Resulting from External Pressure Loading (seen from above) – Steel Specimen 311/10

Fig. 12 – Typical Buckle Pattern at Plastic Collapse, Resulting from External Pressure Loading. Same shell as in Fig. 11 – 311/10.

Fig. 13 – Typical Buckle Pattern in Fully Buckled State, Resulting from External Pressure Loading (seen from above) – Alclad Specimen 421/5.

Fig. 14 – Typical Buckle Pattern at Plastic Collapse, Resulting from External Pressure Loading (seen from above). Same shell as in Fig. 13 – 421/5

Fig. 15 – Ratio of Buckling pressure $p_b$ to that Predicted for Equivalent Cylindrical Shell (Niordson) $p_{th_3}$ for Butt-Welded Steel Cones (and two aluminum alloy cones).

Fig. 16 Ratio of Buckling Pressure $p_b$ to that Predicted for Equivalent Cylindrical Shell (Niordson) $p_{th_3}$ for Adhesive Bonded Alclad Cones.

Fig. 17 – Ratio of Buckling Pressure $p_b$ to that Predicted for Equivalent Cylindrical Shell (Niordson) $p_{th_3}$, Comparison of Results with other Experimental Data.

Fig. 18 – Plastic Collapse Pressure Coefficients.

Fig. 19 – Typical Buckle Pattern for Conical Shell of Large Taper Ratio in Torsion (Plastic Deformation Remaining After Removal from Test Rig) – Alclad Specimen 321/6.

Fig. 20 – Typical Buckle Pattern for Conical Shell of Small Taper Ratio (Plastic Deformation Remaining After Removal from Test Rig) – Steel Specimen 417/6.

Fig. 21 – Typical Experimental Curve of Torque Versus Angle of Twist – Alclad Specimen 321/6.

Fig. 22 – Comparison of Theory and Experiment for Buckling of Conical Shells in Torsion.

Fig. 23 – Typical Buckle Pattern for Conical Shell Under Combined Torsion and External Pressure (Plastic Deformation Remaining After Removal from Test Rig) – Alclad, Specimen 421/9.

Fig. 24 – Experimental Verification of Interaction Curve for Buckling Under Combined Torsion and External Pressure – Shells of Large Taper Ratio.

Fig. 25 – Experimental Verification of Interaction Curve for Buckling Under Combined Torsion and External Pressure – Shells of Small and Medium Taper Ratio.

## S Y M B O L S

| | | |
|---|---|---|
| a | = | distance of the top of a truncated cone from the vertex, along a generator (see Fig. 1). |
| A, B, C, D | = | complex expressions defined by Eqs. (1.46), (1.47), (1.48), and (1.49). |
| $A_n$, $B_n$, $C_n$, $D_n$, $E_n$, $F_n$ | = | displacement coefficients defined by Eq. (1.13). |
| $A_0$ | = | initial out-of-roundness. |
| $b_p$, $c_q$ | = | coefficients defined by Eqs. [3] of Ref. 16. |
| $C_p$ | = | pressure coefficient = $(p/E)\,[12\,(1-\nu^2)/\pi^2]\,(l/h)^2(\rho_{av}/h)$ |
| E | = | modulus of elasticity. |
| $F_1(n)$ etc. $G_1(n,m)$ etc. $K_1(n)$ etc. | = | algebraic expressions involving $\beta$, $\gamma$, t and $\sin\alpha$. |
| h | = | thickness of shell. |
| H, J, K, L, M, N, P, Q, R, T, | = | algebraic expressions involving $\beta$, $\gamma$, t and $\sin\alpha$ defined by Eqs. (1.26) to (1.35). |
| H | = | height of cone = $l\cos\alpha$. |
| $H_2$, $H_2^{-1}$ | = | differential operators defined by Eqs. (1.5) and (1.10). |
| $J_k(n,m)$, $J_p(n,m)$, $J_q(n,m)$ | = | algebraic expressions defined by Eqs. [48], [28] and [29] of Ref. 16. |
| $k_u$ | = | spring constant of the elastic supports in the axial direction. |
| $k_v$ | = | spring constant of the elastic supports in the circumferential direction. |
| $K^4$ | = | $12\,(1-\nu^2)\,(a/h)^2$ |
| l | = | slant length of cone. |

$L_1$ = differential operator defined by Eq. (1.6).

$L_2$ = differential operator defined by Eq. (1.7).

$L_3$ = differential operator defined by Eq. (1.8).

$m$ = integer.

$n$ = integer.

$n_e$ = number of circumferential waves observed in experiment.

$n_{th}$ = number of circumferential waves predicted by theory.

$N$ = number of terms of solution.

$p$ = hydrostatic pressure.

$p_1$ = pressure parameter defined by Eq. [77] of Ref. 1.

$p_{cr.}$ = critical pressure.

$p_0$ = measured pressure at onset of buckling.

$p_f$ = measured pressure when fully buckled.

$p_b$ = buckling pressure, the higher value of $p_0$ or $p_f$.

$p_{th_1}$ = theoretical critical pressure, Singer (Ref. 1).

$p_{th_2}$ = theoretical critical pressure, Seide (Ref. 18).

$p_{th_3}$ = theoretical critical pressure, Niordson (Ref. 26).

$p_p$ = measured pressure at complete plastic collapse.

$p$ = axial force.

$Q(n,m), R(n,m), S(n,m)$ = algebraic expressions defined by Eqs. (1.55), (1.57) and (4.11).

| | | |
|---|---|---|
| $r$ | = | complex number $= \gamma + im\beta$ |
| $R_1$ | = | Radius of small end of truncated cone. |
| $R_2$ | = | Radius of large end of truncated cone. |
| $s$ | = | complex number $= \gamma + in\beta$ |
| $t$ | = | number of circumferential waves. |
| $T$ | = | torque. |
| $\bar{T}$ | = | torque of equivalent cylindrical shell. |
| $T_1$ | = | temperature parameter defined by Eq. [1] of Ref. 16. |
| $U, V$ | = | algebraic expressions, involving $\beta$, $\gamma$, t, n and $\sin\alpha$ defined by Eqs. (1.41) and (1.42). |
| $u^*$ | = | displacement along a generator. |
| $u$ | = | non-dimensional displacement along a generator $= u^*/a$. |
| $v^*$ | = | circumferential displacement. |
| $v$ | = | non-dimensional circumferential displacement $= v^*/a$. |
| $w^*$ | = | radial displacement. |
| $w$ | = | non-dimensional radial displacement $= w^*/a$. |
| $x^*$ | = | axial co-ordinate, along a generator. |
| $x$ | = | non-dimensional axial co-ordinate $= x^*/a$. |
| $x_2$ | = | ratio of the distance of the bottom of a truncated cone from the vertex, to that of the top. |

$\bar{Z}$ = geometrical shell parameter = $(1-\nu^2)^{\frac{1}{2}} (1/\rho_{av})^2$

$\alpha$ = cone angle.

$\beta$ = $(\pi/\lg_e x_2)$ (see Eq. (1.19)).

$\gamma$ = $(1-\nu)/2$ (see Eq. (1.20)).

$\eta$ = axial compression parameter = $(P/E)(K^4/2\pi h\, a \sin\alpha \cos\alpha)$.

$\lambda$ = pressure parameter = $K^4 (p/E)(a/h) \tan\alpha$.

$\lambda_0$ = pressure parameter for zero torque.

$\mu$ = torque parameter = $(K^4/E)(T/a^2 h\, 2\pi \sin^2\alpha)$.

$\mu_0$ = torque parameter for zero pressure.

$\nu$ = Poisson's ratio.

$\rho_{av}$ = mean radius of curvature = $(R_1 + R_2)/2 \cos\alpha$.

$\bar{\sigma}_x, \bar{\sigma}_\phi, \bar{\tau}_{x\phi}$ = membrane stresses of prebuckling state.

$\sigma_x^*, \tau_{x\phi}^*$ = edge stresses due to elastic restraint.

$\phi$ = circumferential co-ordinate.

Subscripts following a comma indicate differentiation.

## SECTION 1

# BUCKLING OF CIRCULAR CONICAL SHELLS UNDER COMBINED TORSION AND EXTERNAL OR INTERNAL PRESSURE

Josef Singer and Menahem Baruch

## INTRODUCTION

In Ref. 1 a method was developed for the analysis of the instability of conical shells under external pressure.

The method is based on a solution of the Donnell type stability equations, derived by Seide (Ref. 2 and 3), and rederived in a modified form to facilitate solution by the Galerkin method, in the presence of slightly relaxed boundary conditions. The solution satisfies the usual simple support conditions regarding the radial deflections, w, rigorously, but implies elastic restraints as far as the axial and circumferential displacements are concerned. However, the constraint on the circumferential, v, displacements is of such a nature that it practically represents the rigid fixation required by the usual simple supports; and the much weaker constraint on the axial, u, displacements (in the direction of the generators) combines with the very small u displacements themselves to a condition approximating freedom from axial restraint. The effect of the u restraint on the instability of cylindrical and conical shells under external pressure was previously investigated and the critical pressures found to differ by $1-2$ percent for typical shells. (Ref. 4 and 5). For the case of instability under torsion, the effect of overall axial constraint was investigated by Donnell (Ref. 6) for cylindrical shells, and found to be negligible. Batdorf (Ref. 7), who compared results calculated under the customary simple support assumptions $u \neq 0$, $v = 0$ with those of Leggett (Ref. 8), for $u = o$, $v = o$, also found close agreement indicating the unimportance of axial constraint.

The method of Ref. 1 is now applied to investigate buckling of thin truncated conical shells under combined torsion and axisymmetrical external or internal pressure.

The problem of buckling of thin conical shells in pure torsion was first treated by Pflüger (Ref. 9), but the solution given there is valid only for shells with small cone angle. Seide (Ref. 10) obtained a more accurate solution which is not restricted to small cone angles. Though the boundary conditions of the present analysis are slightly different to those of Ref. 10, Seide's solution is used for comparison in the limiting case of zero pressure.

## DIFFERENTIAL EQUATIONS, BOUNDARY CONDITIONS AND SOLUTION

The stability equations for a thin conical shell of Refs. 2 and 3 can be written in non-dimension-

al form, as in Ref. 1,

$$(x/\sin^2 \alpha)\, H_2\,(x u) = \cot \alpha\, [L_1(w) - L_2(w)] \tag{1.1}$$

$$(x/\sin^2 \alpha)\, H_2\,(xv) = \cot \alpha\, L_3(w) \tag{1.2}$$

and

$$H_2 \left\{(x/\sin^2 \alpha)\, H_2\,(w) - (K^4/E)\left[x^3 \bar{\sigma}_x w_{,xx} + \bar{\sigma}_\phi [(x/\sin^2 \alpha)\, w_{,\phi\phi} + x^2 w_{,x}] + 2\bar{\tau}_{x\phi} [(x^2/\sin \alpha)\, w_{,x\phi} - (x/\sin \alpha)\, w_{,\phi}]\right]\right\} + K^4 \cos^2 \alpha\, (x^3 w_{,xx})_{,xx} = 0 \tag{1.3}$$

where u, v, and w are the additional displacements caused by buckling

$$K^4 = 12(1-\nu^2)(a/h)^2 \tag{1.4}$$

The operator $H_2$ is defined as

$$H_2(z) = x \sin \alpha\, (x \sin \alpha z_{,xx})_{,xx} + z_{,xx\phi\phi} + x \sin \alpha\, (z_{,\phi\phi}/x \sin \alpha)_{,xx} + (z_{,\phi\phi\phi\phi}/x^2 \sin^2 \alpha) + 2(z_{,\phi\phi}/x^2) - x \sin \alpha (\sin \alpha z_{,x}/x)_{,x} \tag{1.5}$$

and $L_1$, $L_2$ and $L_3$ are further operators defined as

$$L_1(z) = [\nu (\partial/\partial x)\, x - (1+\nu)]\, [x^2 z_{,xx} + x z_{,x} + (1/\sin^2 \alpha)\, z_{,\phi\phi} - z] \tag{1.6}$$

$$L_2(z) = (1/\sin^2 \alpha)\, [(1+\nu)(xz)_{,x} - (3+\nu) z]_{,\phi\phi} \tag{1.7}$$

$$L_3(z) = (1/\sin \alpha)\, [(2+\nu) x^2 z_{,xx} + 3 x z_{,x} + z + (1/\sin^2 \alpha)\, z_{,\phi\phi}]_{,\phi} \tag{1.8}$$

To facilitate solution by the Galerkin method, Eq. (1.3) can be rederived in a modified form as in Ref. 1.

$$(1/x^2 \sin^2 a)\, H_2(w) - K^4 \{(\bar{\sigma}_x/E)\, w_{,xx} + (\bar{\sigma}_\phi/E)[(1/x^2 \sin^2 a)\, w_{,\phi\phi} + (1/x)\, w_{,x}] + 2(\bar{\tau}_{x\phi}/E)[(1/x \sin a)\, w_{,x\phi} - (1/x^2 \sin a)\, w_{,\phi}]\} + (1/x^3) K^4 \cos^2 a\, H_2^{-1}[(x^3 w_{,xx})_{,xx}] = 0 \tag{1.9}$$

where $H_2^{-1}$ is an inverse operator defined by

$$H_2[H_2^{-1}(z)] = z \tag{1.10}$$

The modified equation, Eq. (1.9), has the advantage that it actually represents the radial equilibrium of the forces on an element of the shell, and not a higher order derivative of it. Hence one has no doubt that its Galerkin solution is an upper bound, whereas with Eq. (1.3) this could not be stated with certainty.

The boundary conditions for the buckling displacements for a circular truncated cone which is supported in a manner approximating the conventional simple supports are:

$$w = 0 \qquad \text{at} \qquad x = 1, x_2 \tag{1.11}$$

and

$$w_{,xx} + (\nu/x)\, w_{,x} \qquad \text{at} \qquad x = 1, x_2 \tag{1.12}$$

Instead of the usual requirements that $v = 0$ and $u$ is unrestrained at the end sections, it is here assumed that the displacements in the $u$ and $v$ directions are resisted by elastic supports, as will be shown in detail later.

The solution of Ref. 1 is now extended in a manner suggested by Batdorf for cylindrical shells (Ref. 7). Two formulations of the solution apply to buckling of conical shells in torsion:

$$u = \Im m \left[ \sin t\phi \sum_{n=1,3,\ldots}^{\infty} A_n x^s + \cos t\phi \sum_{n=2,4,\ldots}^{\infty} E_n x^s \right]$$

$$v = \Im m \left[ \cos t\phi \sum_{n=1,3,\ldots}^{\infty} B_n x^s + \sin t\phi \sum_{n=2,4,\ldots}^{\infty} F_n x^s \right]$$

$$w = \Im m \left[ \sin t\phi \sum_{n=1,3,\ldots}^{\infty} C_n x^s + \cos t\phi \sum_{n=2,4,\ldots}^{\infty} D_n x^s \right] \qquad (1.13a)$$

or

$$u = \Im m \left[ \sin t\phi \sum_{n=1}^{\infty} A_n x^s + \cos t\phi \sum_{n=2}^{\infty} E_n x^s \right]$$

$$v = \Im m \left[ \cos t\phi \sum_{n=1}^{\infty} B_n x^s + \sin t\phi \sum_{n=2}^{\infty} F_n x^s \right]$$

$$w = \Im m \left[ \sin t\phi \sum_{n=1}^{\infty} C_n x^s + \cos t\phi \sum_{n=2}^{\infty} D_n x^s \right] \qquad (1.13b)$$

where $C_n$, $D_n$ and $t$ are real, ($t$ is the number of circumferential waves of the buckling deformation), $s$ is the complex number

$$s = \gamma + in\beta \qquad (14.1)$$

$n$ is an integer and the symbol $\Im m$ indicates the imaginary part of the solution.

Restrictions have to be imposed on $n$, in Eqs. (1.13a) or (1.13b), as shown, since only an asymmetric deflection function can represent the torsional displacement. The complete series, Eqs. (1.13a) with no restrictions on $n$, or Eqs. (1.13b) commencing from $n = 1$ in both terms of each function, do not represent a possible torsional displacement, because then the two terms of each function would be equal, with no preference for the $\sin t\phi$ or $\cos t\phi$ term. In Batdorf's formulation for cylindrical shells (Eq. [16] of Ref. 7 or Eq. [6] of Ref. 11) no similar restrictions were necessary, as they are automatically introduced by the orthogonality relations. However, Flügge (Ref. 12) introduces restrictions similar to those of Eqs. (1.13a) in his solution for

cylindrical shells as reasonable and advisable.

In practice, finite series replace Eqs. (1.13a) and (1.13b). In the first formulation n varies from 1 to N for the first terms of Eqs. (1.13a) and from 2 to N ± 1 for the second terms. In the second formulation n varies from 1 to N or N− 1 for the first terms of Eqs. (1.13b) and 2 to N for the second terms. It should be noted that for pure torsion loading, the first formulation converges more rapidly, but the second formulation is more general and applies also to combined loadings.

It may be pointed out that some alternative series may be written instead of Eqs. (1.13b) for the second formulation, since the essential quality is the asymmetry introduced. For example, n could commence at 1 for both terms, leaving out any one term of the first or second group to introduce the asymmetry. However, the form of Eqs. (1.13b) is most the orderly and convenient one, and for finite series, the other forms yield either identical results or results which differ only slightly; though one can arrange sometimes special forms which converge more rapidly, if one remembers that the terms of Eqs. (1.13a) are the most important ones for the buckling in torsion.

Now, if the complex functions, whose imaginary parts represent the assumed solution, Eqs. (1.13a) or (1.13b), satisfy the differential equations, Eqs. (1.1) and (1.2), the equations will also be satisfied by the imaginary parts. Substitution of the complex functions of Eqs. (1.13a) or (1.13b) into Eqs. (1.1) and (1.2) yields, therefore

$$A_n = \frac{\cos\alpha \sin\alpha\,(s-1)\,[t^2 + (s+1)\,(\nu s - 1)\sin^2\alpha]}{t^4 - 2t^2\,(s^2+1)\sin^2\alpha + (s^2-1)^2\sin^4\alpha}\,C_n \tag{1.15}$$

$$B_n = \frac{-t\cos\alpha\,\{t^2 - \sin^2\alpha\,[s^2\,(2+\nu) + s\,(1-\nu) + 1]\}}{t^4 - 2t^2\,(s^2+1)\sin^2\alpha + (s^2-1)^2\sin^4\alpha}\,C_n \tag{1.16}$$

and similarly

$$E_n = \frac{\cos\alpha \sin\alpha\,(s-1)\,[t^2 + (s+1)\,(\nu s - 1)\sin^2\alpha]}{t^4 - 2t^2\,(s^2+1)\sin^2\alpha + (s^2-1)^2\sin^4\alpha}\,D_n \tag{1.17}$$

$$F_n = \frac{t \cos \alpha \{ t^2 - \sin^2 \alpha [ s^2 (2 + \nu) + s (1 - \nu) + 1 ] \}}{t^4 - 2t^2 (s^2 + 1) \sin^2 \alpha + (s^2 - 1)^2 \sin^4 \alpha} D_n \tag{1.18}$$

To ensure compliance with the boundary conditions Eqs. (1.11) and (1.12), one has to define $\beta$ as

$$\beta = \pi / l g x_2 \tag{1.19}$$

and $\gamma$ as

$$\gamma = (1 - \nu)/2 \tag{1.20}$$

as in Ref. 1.

## EFFECT OF ELASTIC RESTRAINT

The axial and circumferential displacements do not vanish, but the edges are assumed to be elastically restrained. It is assumed that the elastic restraints come into action only at the onset of buckling. The displacements prior to buckling are not restrained, and the stress prior to buckling, does therefore not include any elastic restraint. As a result of the assumed buckling displacements Eqs. (1.13) restraining stresses $\sigma_x^*$ and $r_{x\phi}^*$ appear in the elastic supports.

$$\sigma_x^* = [E/(1 - \nu^2)] [u_{,x} + (\nu/x \sin \alpha) (v_{,\phi} + u \sin \alpha - w \cos \alpha)]$$

$$= E \sin \alpha \cos \alpha \, \Im m \sum_n x^{s-1} \frac{\{ s (s-1) [ t^2 - (s + 1) \sin^2 \alpha ] \}}{[t^4 - 2t^2 (s^2 + 1) \sin^2 \alpha + (s^2 - 1)^2 \sin^4 \alpha]} [C_n \sin t\phi + D_n \cos t\phi] \tag{1.21}$$

and

$$r^*_{x\phi} = [E/2(1+\nu)]\,[v_{,x} - (1/x \sin\alpha)(v \sin\alpha - u_{,\phi})]$$

$$= Et\cos t\phi \cos\alpha\, \Im m \sum_n x^{s-1} \frac{s^2(s-1)\sin^2\alpha}{[t^4 - 2t^2(s^2+1)\sin^2\alpha + (s^2-1)^2 \sin^4\alpha]} C_n \cos t\phi - D_n \sin t\phi] \tag{1.22}$$

The spring constants of the elastic supports can now be defined as

$$k_u = \sigma^*_x/au \qquad \text{and} \qquad k_v = r^*_{x\phi}/av \tag{1.23}$$

Substitutions yield for $x = 1, x_2$

$$k_u = (E/ax) \frac{\sum_n \cos(n\beta \lg x)\,[(MQ - PN)/(M^2+N^2)]\,(C_n \sin t\phi + D_n \cos t\phi)}{\sum_n \cos(n\beta \lg x)\,[(MT - RN)/(M^2+N^2)]\,(C_n \sin t\phi + D_n \cos t\phi)} \tag{1.24}$$

and

$$k_v = -\left(\frac{E \sin^2\alpha}{ax}\right) \frac{\sum_n \cos(n\beta \lg x)\,[(MJ - HN)/(M^2+N^2)]\,(C_n \cos t\phi - D_n \sin t\phi)}{\sum_n \cos(n\beta \lg x)\,[(ML - KN)/(M^2+N^2)]\,(C_n \cos t\phi - D_n \sin t\phi)} \tag{1.25}$$

where

$$M = t^4 - 2t^2(\gamma^2 - n^2\beta^2 + 1)\sin^2\alpha + [(n^2\beta^2 + 1 - \gamma^2)^2 - 4\gamma^2 n^2 \beta^2]\sin^4\alpha \tag{1.26}$$

$$N = 4\gamma n\beta\,[(\gamma^2 - n^2\beta^2 - 1)\sin^2\alpha - t^2]\sin^2\alpha \tag{1.27}$$

$$P = [\gamma(\gamma-1) - n^2\beta^2]\,t^2 + \gamma\,[3n^2\beta^2 - \gamma^2 + 1]\sin^2\alpha \tag{1.28}$$

$$Q = n\beta\,[2\gamma - 1)\,t^2 + (n^2\beta^2 - 3\gamma^2 + 1)\sin^2\alpha] \tag{1.29}$$

$$R = (\gamma-1)\,t^2 + [(-2\gamma^4 + \gamma^3 + \gamma^2 - \gamma + 1) + (6\gamma^2 - 3\gamma + 1)\,n^2\beta^2]\sin^2\alpha \tag{1.30}$$

$$T = n\beta\,\{t^2 + [(-6\gamma^3 + 3\gamma^2 - 1) - (1 - 2\gamma)\,n^2\beta^2]\sin^2\alpha\} \tag{1.31}$$

$$H = \gamma^3 - \gamma^2 + (1 - 3\gamma)\, n^2 \beta^2 \tag{1.32}$$

$$J = n\beta\,(3\gamma^2 - 2\gamma - n^2 \beta^2 \tag{1.33}$$

$$K = t^2 - [(-2\gamma^3 + 5\gamma^2 + 1) - (3 - 2\gamma)\, n^2 \beta^2]\, \sin^2 \alpha \tag{1.34}$$

$$L = -n\beta\,(2 - \gamma)\, 4\gamma \sin^2 \alpha \tag{1.35}$$

It should be noted that the spring constants $k_u$ and $k_v$ have the dimensions of stress per inch (psi per inch), and that the restrictions on the values $n$ imposed in Eqs. (1.13a) and (1.13b) apply to all the expressions.

To obtain an estimate of the order of magnitude of the spring constants, the first approximation (the solution with the smallest number of terms) suffices. For both formulations this is the solution with $n = 1$ in the first terms of Eqs. (1.13) and $n = 2$ in the second terms.

The typical shells of the following dimensions are considered for the purpose of this estimate (see Fig. 2):

| (a) | | (b) | |
|---|---|---|---|
| $\alpha$ | $= 30°$ | $\alpha$ | $= 40°$ |
| a | $= 57.59"$ | a | $= 7.78"$ |
| $x_2$ | $= 1.5$ | $x_2$ | $= 2.5$ |
| h | $= 0.1"$ | h | $= 0.0158"$ |

Taking $\nu = 0.3$ and $n = 1$ and 2, in accordance with the restrictions of Eqs. (1.13a) and (1.13b), one obtains at $x = 1$ (where the largest values occur) the following mean values of the spring constants:

| SHELL | (a) | (b) |
|---|---|---|
| $k_u/E$ | $-0.0059$ | $-0.0420$ |
| $k_v/E$ | $-2.63$ | $-4.55$ |

At $x = x_2$, the spring constants are $(1/x_2)$ times the above values.

It should be noted that the spring constants computed from Eqs. (1.24) and (1.25) are functions of $\phi$ , which go to infinity wherever u or v vanishes. The reason for this behaviour is the fact that the restraints introduced by the solution are not physical springs, and yield finite restraining forces even at points of vanishing displacements. Since however at such points no work is done by those forces, the analysis is not affected. The mean integrated effects of the restraints do behave as springs (though negative ones) and therefore the mean spring coefficients are considered.

As for external pressure, the spring constants in the circumferential direction, $k_v$ , are very large, and hence the solution approaches the realistic condition of vanishing circumferential displacement ($v = 0$) at the supported ends. The spring constants in the axial direction, $k_u$ , although about 1/100 of $k_v$ , are still large, while the usual conditions of simple supports (no restraint on u) would be approximated by a small spring constant. However, since the u displacements are much smaller that the w displacements the restraining axial forces will be small, although $k_u$ is of considerable magnitude. Note that $k_u$ is negative. Hence the solution introduces a negative elastic restraint which would tend to reduce the stiffness of the shell. The order of magnitude of the spring coefficients is the same as for external pressure. Shell (b) has larger spring coefficients than the typical shells investigated in Ref. 1. However, from Ref. 5, the effect is seen to be less than 4% even for such "strong" springs.

It seems reasonable to assume that the effect of axial constraint on the instability in torsion should be even less than that under external pressure loading. Hence the effect of the springs can be neglected as in Ref. 1.

## BUCKLING UNDER UNIFORM HYDROSTATIC EXTERNAL OR INTERNAL PRESSURE AND TORSION

The basic equilibrium conditions of the conical shell yield the following relations for the membrane stresses in the case of external or internal hydrostatic pressure loading and torsion.

$$\bar{\sigma}_x = \mp (p/2)\,(a/h)\,x \tan \alpha \tag{1.36}$$

$$\bar{\sigma}_\phi = \mp p\,(a/h)\,x \tan \alpha \tag{1.37}$$

$$\bar{\tau}_{x\phi} = T/a^2 h\, 2\pi x^2 \sin^2 \alpha \tag{1.38}$$

In Eqs. (1.36) and (1.37) the minus sign is for external pressure loading and the plus sign for internal pressure.

If it is assumed that the boundary conditions come into action only after the prebuckling stress state has been established, these stresses satisfy the equilibrium conditions exactly. If the boundary conditions are taken into account, additional bending stresses appear, which however are significant only in the neighbourhood of the supports.

Assuming now that for the buckling analysis the prebuckling stress is represented satisfactorily by Eqs. (1.36) to (1.38), the modified third stability equation, Eq. (1.9), becomes

$$\begin{aligned}(1/x^2 \sin^2 \alpha)\, H_2(w) &\pm K^4 (p/E)(a/h) \tan \alpha \,[(x/2)\, w_{,xx} + (1/x \sin^2 \alpha)\, w_{,\phi\phi} + (1/x)\, w_{,x}] \\ &- 2\,(K^4/E)\,(T/a^2 h\, 2\pi \sin^2 \alpha)\,[(1/x^3 \sin \alpha)\, w_{,x\phi} - (1/x^4 \sin \alpha)\, w_{,\phi}] \\ &+ (1/x^3)\, K^4 \cos^2 \alpha\, H_2^{-1}\,[(x^3 w_{,xx})_{,xx}] = 0\end{aligned} \tag{1.39}$$

The buckling load is obtained from the requirement that the solution proposed in Eq. (1.13) must satisfy Eq. (1.39), this requirement leads to

$$\begin{aligned}\Im m \sum_n \Big\{ C_n \Big\{ &\sin t\phi \Big\{ x^{s-4} \{ s^2 (s-2)^2 - 2(t^2/\sin^2 \alpha)\,[(s-1)^2 + 1] + (t^4/\sin^4 \alpha) \} \\ &+ K^4 (p/E)(a/h) \tan \alpha\, x^{s-1} \{ [s(s+1)/2] - (t^2/\sin^2 \alpha) \} \\ &+ K^4 \cos^2 \alpha\, x^{s-2} (U^2 + V^2)^{-1} s^2 (s^2 - 1)(U - iV) \Big\} \\ &- \cos t\phi\, [(K^4/E)(T/a^2 h\, 2\pi \sin^2 \alpha)\, x^{s-4}\, 2(t/\sin \alpha)(s-1)] \Big\}\end{aligned}$$

$$+ D_n \Big\{ \cos t\phi \Big\{ x^{s-4} \{ s^2 (s-2)^2 - 2(t^2/\sin^2 \alpha) [(s-1)^2 + 1] + (t^4/\sin^4 \alpha) \}$$

$$+ K^4 (p/E) (a/h) \tan \alpha \; x^{s-1} \{ [s(s+1)/2] - (t^2/\sin^2 \alpha) \}$$

$$+ K^4 \cos^2 \alpha \, x^{s-2} (U^2 + V^2)^{-1} s^2 (s^2 - 1) (U - iV) \Big\}$$

$$+ \sin t\phi \{ (K^4/E) (T/a^2 h \, 2\pi \sin^2 \alpha) \, x^{s-4} \, 2(t/\sin \alpha) (s-1) \} \Big\} \Big\} \tag{1.40}$$

where

$$U = \sin^2 \alpha [(\gamma^2 - 1)^2 - 2(3\gamma^2 - 1) n^2 \beta^2 + n^4 \beta^4] - 2t^2 (\gamma^2 + 1 - n^2 \beta^2) + (t^4/\sin^2 \alpha) \tag{1.41}$$

$$V = 4\gamma n \beta [\sin^2 \alpha (\gamma^2 - 1 - n^2 \beta^2) - t^2] \tag{1.42}$$

and the summation must be carried out over all integral values of n, in accordance with the restrictions of Eqs. (1.13a) or (1.13b).

Equation (1.40) will be evaluated by the Galerkin method. The left hand side of the equation will be multiplied once by $\Im m [x^r \sin t\phi] \times \sin \alpha \, dx \, d\phi$ and once by $\Im m [x^r \cos t\phi] \times \sin \alpha \, dx \, d\phi$, and the products will be integrated from 1 to $x_2$ and from 0 to $2\pi$, where

$$r = \gamma + im\beta \tag{1.43}$$

and m is an integer.

Two sets of Galerkin integrals are obtained

$$\int_0^{2\pi} \sin^2 t\phi \sin\alpha \int_1^{x_2} \sum_n x^\gamma \sin(m\beta \lg x) \Big\{ C_n \big[\cos(n\beta \lg x)\,[x^{\gamma-4}\,\Im m(A) + x^{\gamma-2}\,\Im m(B) + x^{\gamma-1}\,\Im m(C)] + \sin(n\beta \lg x)\,[x^{\gamma-4}\,\Re(A) + x^{\gamma-2}\,\Re(B) + x^{\gamma-1}\,\Re(C)]\big] + D_n \big[\cos(n\beta \lg x)[x^{\gamma-4}\,\Im m(D)] + \sin(n\beta \lg x)\,[x^{\gamma-4}\,\Re(D)]\big] \Big\} x\,dx\,d\phi = 0 \tag{1.44}$$

and

$$\int_0^{2\pi} \cos^2 t\phi \sin\alpha \int_1^{x_2} \sum_n x^\gamma \sin(m\beta \lg x) \Big\{ D_n \big[\cos(n\beta \lg x)\,[x^{\gamma-4}\,\Im m(A) + x^{\gamma-2}\,\Im m(B) + x^{\gamma-1}\,\Im m(C)] + \sin(n\beta \lg x)\,[x^{\gamma-4}\,\Re(A) + x^{\gamma-2}\,\Re(B) + x^{\gamma-1}\,\Re(C)]\big] + C_n \big[\cos(n\beta \lg x)\,[x^{\gamma-4}\,\Im m(D)] + \sin(n\beta \lg x)\,[x^{\gamma-4}\,\Re(D)]\big] \Big\} x\,dx\,d\phi = 0 \tag{1.45}$$

where, as in Ref. 1,

$$A = s^2 (s-2)^2 - 2(t^2/\sin^2\alpha)\,[(s-1)^2 + 1] + (t^4/\sin^4\alpha) \tag{1.46}$$

$$B = K^4 \cos^2\alpha\,(U^2 + V^2)^{-1}\, s^2 (s^2 - 1)\,(U - iV) \tag{1.47}$$

$$C = \pm K^4 (p/E)(a/h) \tan\alpha \big[\,[s(s+1)/2] - (t^2/\sin^2\alpha)\big] \tag{1.48}$$

and

$$D = (K^4/E)(T/a^2 h\, 2\pi \sin^2\alpha)\, 2(t/\sin\alpha)(s-1) \tag{1.49}$$

After integration and some manipulations, Eqs. (1.44) and (1.45) become

$$\sum_n \Big\{ C_n \{[(-1)^{m+n} x_2^{2\gamma-2} - 1]\, G_1(n,m) + K^4 \cos^2\alpha\, [(-1)^{m+n} x_2^{2\gamma} - 1]\, G_2(n,m)$$
$$\pm K^4 [(-1)^{m+n} x_2^{2\gamma+1} - 1]\, G_3(n,m)\,(p/E)\,(a/h)\tan\alpha\}$$
$$+ D_n \{[(-1)^{m+n} x_2^{2\gamma-2} - 1]\, G_4(n,m)\,(K^4/E)\,(T/a^2 h\, 2\pi \sin^2\alpha)\}\Big\} = 0 \qquad (1.50)$$

$$\sum_n \Big\{ D_n \{[(-1)^{m+n} x_2^{2\gamma-2} - 1]\, G_1(n,m) + K^4 \cos^2\alpha\, [(-1)^{m+n} x_2^{2\gamma} - 1]\, G_2(n,m)$$
$$\pm K^4 [(-1)^{m+n} x_2^{2\gamma+1} - 1]\, G_3(n,m)\,(p/E)\,(a/h)\tan\alpha\}$$
$$- C_n \{[(-1)^{m+n} x_2^{2\gamma-2} - 1]\, G_4(n,m)\,(K^4/E)\,(T/a^2 h\, 2\pi \sin^2\alpha)\}\Big\} = 0 \qquad (1.51)$$

The symbols $G(n,m)$ denote values of G functions for a particular n and m. The functions $G_1$, $G_2$ and $G_3$ are given by Eqs. (64), (65) and (66) of Ref. 1 (see also Appendix A) and

$$G_4(n,m) = K_1(n)\left[\frac{m+n}{4(\gamma-1)^2 + (m+n)^2\beta^2} + \frac{m-n}{4(\gamma-1)^2 + (m-n)^2\beta^2}\right]$$
$$+ K_2(n)\left[\frac{1}{4(\gamma-1)^2 + (m+n)^2\beta^2} - \frac{1}{4(\gamma-1)^2 + (m-n)^2\beta^2}\right] \qquad (1.52)$$

where

$$K_1(n) = 2(n t \beta^2/\sin\alpha) \qquad (1.53)$$

$$K_2(n) = 4(\gamma-1)^2 (t/\sin\alpha) \qquad (1.54)$$

Note that in Eqs. (1.50) and (1.51) the sign of the third term is plus for external pressure and minus for internal pressure.

For a fixed value of m, Eqs. (1.50) and (1.51) are linear equations in terms of the coefficients $C_n$ and $D_n$. The load terms also appear linearly in the equations. If m is allowed to vary in the

same way as n, the critical value of the torque for a given external or internal pressure, or the critical external pressure for a given torque, can be calculated from the vanishing of the determinant whose elements are the multipliers of the coefficients $C_n$ and $D_n$.

If one writes

$$Q(n,m) = [(-1)^{m+n} x_2^{2\gamma-2} - 1] G_1(n,m) + K^4 \cos^2 \alpha [(-1)^{m+n} x_2^{2\gamma} - 1] G_2(n,m)$$

$$\pm \lambda [(-1)^{m+n} x_2^{2\gamma+1} - 1] G_3(n,m) \tag{1.55}$$

where $\lambda$ is a pressure parameter defined by

$$\lambda = K^4 (p/E)(a/h) \tan \alpha \tag{1.56}$$

and

$$R(n,m) = \mu [(-1)^{m+n} x_2^{2\gamma-2} - 1] G_4(n,m) \tag{1.57}$$

where $\mu$ is a torque parameter defined by

$$\mu = (K^4/E)(T/a^2 h\, 2\pi \sin^2 \alpha) = (K^4/E) \tau_{max} \tag{1.58}$$

the following linear equations are obtained:

In the first formulation, Eqs. (1.13a),

$$Q(1,1) C_1 + Q(3,1) C_3 + \ldots + Q(N,1) C_N + R(2,1) D_2 + R(4,1) D_4 + \ldots + R(N \pm 1,1) D_{N\pm1} = 0$$

$$Q(1,3) C_1 + Q(3,3) C_3 + \ldots + Q(N,3) C_N + R(2,3) D_2 + R(4,3) D_4 + \ldots + R(N \pm 1,3) D_{N\pm1} = 0$$

$$\vdots$$

$$Q(1,N) C_1 + Q(3,N) C_3 + \ldots + Q(N,N) C_N + R(2,N) D_2 + R(4,N) D_4 + \ldots + R(N\pm1,N) D_{N\pm1} = 0$$

$$-R(1,2)\,C_1 - R(3,2)\,C_3 - \ldots - R(N,2)\,C_N + Q(2,2)\,D_2 + Q(4,2)\,D_4 + \ldots + Q(N\pm1,2)\,D_{N\pm1} = 0$$

$$-R(1,4)\,C_1 - R(3,4)\,C_3 - \ldots - R(N,4)\,C_N + Q(2,4)\,D_2 + Q(4,4)\,D_4 + \ldots + Q(N\pm1,4)\,D_{N\pm1} = 0$$

$$\vdots$$

$$-R(1,N\pm1)\,C_1 - R(3,N\pm1)\,C_3 - \ldots - R(N,N\pm1)\,C_N + Q(2,N\pm1)\,D_2 + Q(4,N\pm1)\,D_4 + \ldots + Q(N\pm1,N\pm1)\,D_{N\pm1} = 0 \qquad (1.59)$$

and in the second formulation, Eqs. (1.13b),

$$Q(1,1)\,C_1 + Q(2,1)\,C_2 + \ldots + Q(N,1)\,C_N + R(2,1)\,D_2 + R(3,1)\,D_3 + \ldots + R(N,1)\,D_N = 0$$

$$Q(1,2)\,C_1 + Q(2,2)\,C_2 + \ldots + Q(N,2)\,C_N + R(2,2)\,D_2 + R(3,2)\,D_3 + \ldots + R(N,2)\,D_N = 0$$

$$\vdots$$

$$Q(1,N)\,C_1 + Q(2,N)\,C_2 + \ldots + Q(N,N)\,C_N + R(2,N)\,D_2 + R(3,N)\,D_3 + \ldots + R(N,N)\,D_N = 0$$

$$-R(1,2)\,C_1 - R(2,2)\,C_2 - \ldots - R(N,2)\,C_N + Q(2,2)\,D_2 + Q(3,2)\,D_3 + \ldots + Q(N,2)\,D_N = 0$$

$$-R(1,3)\,C_1 - R(2,3)\,C_2 - \ldots - R(N,3)\,C_N + Q(2,3)\,D_2 + Q(3,3)\,D_3 + \ldots + Q(N,3)\,D_N = 0$$

$$\vdots$$

$$-R(1,N)\,C_1 - R(2,N)\,C_2 - \ldots - R(N,N)\,C_N + Q(2,N)\,D_2 + Q(3,N)\,D_3 + \ldots + Q(N,N)\,D_N = 0 \qquad (1.60)$$

For any given pressure, the lowest eigenvalue $\mu$ of the determinant of the coefficients of $C_n$ and $D_n$ of Eqs. (1.59) or (1.60) yields the critical torque. For any given torque the lowest eigenvalue $\lambda$ of that determinant yields the critical external pressure. It should be noted that the value of t (the

number of circumferential waves into which the shell buckles) which "minimizes" the critical load has to be used.

It may be noted that the determinant of the coefficients of Eqs. (1.59) can be obtained directly from these equations, which result when m varies in the same manner as n; or from a larger set, which appears when m is allowed to take all values from one to N (or N + 1), after rearranging of rows and columns as in Ref. 11.

T A B L E 1

Critical Shear Stress for Torsion Alone

| Shell | (a) | | (b) | | (c) | |
|---|---|---|---|---|---|---|
| $\alpha$ | $30^0$ | | $40^0$ | | $40^0$ | |
| $x_2$ | 1.5 | | 2.5 | | 6.35 | |
| $\psi$ | 0.333 | | 0.6 | | 0.843 | |
| a | 57.59 in. | | 7.78 in | | 3.06 in | |
| h | 0.1 in. | | 0.0158 in | | 0.0158 in | |
| $\nu$ | 0.3 | | 0.3 | | 0.33 | |
| Order of Determinant | Critical Maximum Shear Stress $(\tau_{max.cr.}/E) \times 10^6$ | | | | | |
| | With Eqs. (1.13a) | With Eqs. (1.13b) | With Eqs. (1.13a) | With Eqs. (1.13b) | With Eqs. (1.13a) | With Eqs. (1.13b) |
| 2 | 915 | 915 | 683 | 683 | 2325 | 2325 |
| 3 | 743 | 914 | 548 | 680 | 1808 | 2298 |
| 4 | 735 | 910 | | | | |
| 5 | 732 | 742 | 539 | 545 | 1735 | 1780 |
| 6 | | 737 | | | | |
| 7 | | 731 | | | | |
| 8 | | 728 | | | | |
| 9 | | 727 | | 540 | | 1540 |
| Approx. Critical Stress (Seide, Ref. 10) | 722 | | 520 | | 1520 | |

The critical torques, in the case of pure torsion loading, and the corresponding critical shear

stresses, were calculated with both formulations, Eqs. (1.13a) and (1.13b), for the typical shells of Fig. 2. The maximum critical shear stresses $\tau_{max.cr.}$ are tabulated in Table 1, and are compared with the approximate formula of Ref. 10. The results indicate rapid convergence.

As in the case of buckling under external pressure, convergence is slower for longer or shallower shells, i.e. those with larger taper ratio ($\psi$). For shell (a), a typical short shell, a 3 × 3 stability determinant of the first formulation – Eqs. (1.13a), or a 5 × 5 determinant of the second formulation – Eqs. (1.13b), yields a critical shear stress which is only about 2.5% too high. For shell (b), a typical medium shell, a 3 × 3 determinant of the first formulation, or a 5 × 5 determinant of the second formulation, yields a critical shear stress which is about 4.5% too high. For shell (c), a typical long shell of large taper ratio, determinants of similar order yield critical stresses about 17% and 15.5% too high, respectively. The first formulation, Eqs. (1.13a), is indeed superior for pure torsion loading. However, for longer and shallower shells, of larger taper ratio, for which the buckling deformation differs considably from that of cylindrical shells (see Section 3 of this report, or Ref. 19 for experimental evidence), the second formulation improves the solution considerably for the same range of n, though with higher order determinants.

For practical purposes, a 3 term solution, with n taking values up to 3, which corresponds to a 3 × 3 stability determinant in the first formulation or a 5 × 5 one in the second one, suffices unless the taper ratio $\psi$ of the shell is large.

The critical shear stresses obtained from higher order determinants are practically identical to those obtained by the method of Ref. 10, though Seide's boundary conditions differ slightly. Similar agreement was found in the case of external pressure (see Ref. 1). The corresponding critical torsion ratios ($T/\bar{T}\cos^2\alpha$) are also plotted in Fig. 22.

The maximum critical shear stress in the presence of external pressure is then calculated for the same typical shells. The ratio of critical shear stress to that for pure torsion are tabulated in Table 2. The second approximation and then a solution obtained with a 7th or 9th order determinant are given. The second formulation, Eqs. (1.13b), is used here. The results are also compared with a semi-empirical interaction formula obtained by Crate, Batdorf, and Baab (Ref. 13) for cylindrical shells under combined internal pressure and torsion, which was confirmed by the theoretical analysis of Hopkins and Brown (Ref. 14), and was reconfirmed also for combined external pressure and torsion, both theoretically

and experimentally, by Suer and Harris (Ref. 15). This formula can be written

$$(\lambda/\lambda_0) + (\mu/\mu_0)^2 = 1 \tag{1.61}$$

where $\lambda_0$ and $\mu_0$ are the critical pressure parameter for zero torque and the critical torque parameter for zero pressure, respectively.

T A B L E 2

Critical Shear Stress Ratio for Torsion and Uniform External or Internal Pressure

| | | | | $\tau_{cr.}/\tau_{cr.\ torsion\ alone}$ or $(\mu/\mu_0)$ | | | | |
|---|---|---|---|---|---|---|---|---|
| Shell | $\alpha$ | $x_2$ | Order of Determinant | EXTERNAL PRESSURE $(\lambda/\lambda_0)$ | | | | |
| | | | | 0 | 0.25 | 0.5 | 0.75 | 1.0 |
| (a) | $30^0$ | 1.5 | 3 | 1.0 | 0.827 | 0.646 | 0.440 | 0 |
| | | | 7 | 1.0 | 0.866 | 0.713 | 0.504 | 0 |
| (b) | $40^0$ | 2.5 | 3 | 1.0 | 0.832 | 0.650 | 0.436 | 0 |
| | | | 7 | 1.0 | 0.874 | 0.725 | 0.526 | 0 |
| | | | 9 | 1.0 | | 0.735 | | 0 |
| (c) | $40^0$ | 6.35 | 3 | 1.0 | 0.861 | 0.709 | 0.490 | 0 |
| | | | 7 | 1.0 | 0.903 | 0.815 | 0.711 | 0 |
| Semi-Empirical Interaction formula of Ref. 13. | | | | 1.0 | 0.865 | 0.707 | 0.500 | 0 |

The computations and interaction curves can easily be extended to internal pressures. Such calculations are in progress now.

The results are plotted in Fig. 3. For cones with small or medium taper ratio, whose buckling behaviour is similar to that of cylindrical shells, the interaction curves are also very similar. For shell (a) the curve is practically identical to the semi-empirical formula of Ref. 13, Eq. (1.61), and for shell (b) it differs only slightly (by about 2.5% for $\lambda/\lambda_0 = 0.5$ with a $7 \times 7$ determinant). A sample calculation with a $9 \times 9$ determinant indicated a slightly larger difference (4% at the same point). The typical shell of large taper ratio, shell (c), whose buckling behaviour differs considerably from that of

a cylindrical shell (see for example Fig. 19 and Fig. 23), exhibits also an entirely different interaction curve (for example, $\mu/\mu_0$ is about 14% higher than that for a cylindrical shell at $\lambda/\lambda_0 = 0.25$).

More extensive computations are required to establish a set of reliable interaction curves for conical shells, but the present calculations demonstrate clearly that for external pressure use of Eq. (1.61) for conical shells will result in conservative estimates, especially so for (a) shell of large taper ratio. It should be noted,however, that preliminary calculations have shown that this is not the case for internal pressure !

## BUCKLING UNDER LATERAL PRESSURE VARYING IN THE AXIAL DIRECTION, AXISYMMETRICAL TEMPERATURE DISTRIBUTIONS AND TORSION

Since the above analysis is linear, it may be extended to include other loadings which can be expected to have buckling displacements represented by Eqs. (1.13). If the more general second formulation of Eqs. (1.13b) is considered, the analysis applies to combined loadings of lateral pressure varying in the axial direction, thermal stresses caused by axisymmetrical temperature distributions and torsion. One has only to modify the load terms in Eqs. (1.60) in an appropriate manner, i.e. to replace $Q(n,m)$ of Eq. (1.55) by

$$\begin{aligned}\bar{Q}(n,m) = {} & [(-1)^{m+n} x_2^{2\gamma-2} - 1]\, G_1(n,m) + K^4 \cos^2\alpha\, [(-1)^{m+n} x_2^{2\gamma} - 1]\, G_2(n,m) \\ & \pm K^4 (p_1/E)(n/h) \tan\alpha\, J_k(n,m)\, [(-1)^{m+n} x_2^{2\gamma+k} - 1] \\ & + (K^4/E)\, T_1 \Big[ \sum_{p=0}^{P} b_p\, J_p(n,m)\, [(-1)^{m+n} x_2^{2\gamma+p} - 1] \\ & \qquad + \sum_{q=0}^{Q} c_q\, J_q(n,m)\, [(-1)^{m+n} x_2^{2\gamma+q} - 1] \Big] \end{aligned} \tag{1.62}$$

Where $p_1$ and $J_k$ are given by Eqs. [77] and [94] of Ref. 1 (or Eqs. [45] and [48] of Ref. 16), and $T_1$, $b_p$, $c_q$, $J_p$ and $J_q$ are given by Eqs. [1], [3], [28] and [29] of Ref. 16 respectively.

# SECTION 2

## EXPERIMENTAL INVESTIGATION OF THE BUCKLING OF CONICAL SHELLS UNDER UNIFORM HYDROSTATIC PRESSURE

Josef Singer and Abraham Eckstein

# INTRODUCTION

In Ref. 17 the results of an experimental investigation of the instability of thin truncated conical shells under uniform external pressure, carried out at the Technion, were reported. Test of 71 shells made of a weldable aluminum alloy were described and correlated with the theoretical analysis of Refs. 1 and 18, and also compared with other experimental investigations (Refs. 19–21). The theoretical analyses were verified in general by the test results, though there was considerable scatter. Careful analysis of the causes of scatter however indicated a better fit of the theoretical curve than was at first apparent.

In order to investigate further some of the causes of scatter, and in order to consolidate the experimental verification of the theory, two additional series of tests were carried out: One with butt-welded stainless steel specimens (and a few butt-welded aluminum alloy cones), and one with bonded (lap-jointed) alclad specimens.

33 truncated cones tested under uniform external pressure covering the $(\rho_{av}/h)$ range (mean radius of curvature to thickness ratios) 240 – 725.

# TEST APPARATUS AND PROCEDURE

The test rig used in the earlier investigation (Ref. 17) is also employed here. It is shown in Fig. 3 and 4, after it has been adapted for combined torsion and external pressure loading, and is described in Section 3. The rig for external pressure loading consists of: a pressure vessel with end fixtures for the specimens, a pressurizing system, which in the present tests is throttled air from a central compressed air supply, and a pressure measuring system. The latter includes a head of mercury (or of alcohol, for lower pressures) as well as a sensitive Statham pressure gage (which records via an unbonded strain gage). With this duplication, continuous calibration of the Statham gage during the test is possible, while utilizing its sensitivity.

As in earlier tests (Ref. 17), simple support conditions are approached as far as possible. The end fittings here have a circular profile and the outer rings have O-seals at the contact line, so that the

rotation of the generators is only slightly restrained, see Fig. 4. The top and bottom fixtures are similar. The displacement along the generators is restrained by the friction of the seal and inner ring, but the ends are free to move axially as a whole. Since the effect of restraint along the generators on the buckling pressure is very small (see Ref. 5), while restraint of edge rotation has a significant effect on it, the test boundary conditions appear to be a fair approximation to the theoretical simple support conditions

$$\left.\begin{aligned} w &= 0 \\ v &= 0 \\ u &\neq 0 \quad (N_x = 0) \\ \text{and} \quad w_{,xx} &+ (\nu/x)\, w_{,x} = 0 \end{aligned}\right\} \quad \text{at top and bottom end fixtures} \tag{2.1}$$

The second series of tests confirm this very clearly, as discussed in detail below.

The test procedure was similar to that employed in the earlier tests, except that the visual indication disc (Fig. 4 of Ref. 17) was not used in most of the present tests. The out-of-roundness was measured, with a dial gage mounted on a rotary arm (see Fig. 6), at a radius slightly larger than the mean, where the maximum buckling deflection was expected. For some cones these measurements were also taken at two or three radii and compared. The out-of-roundness measurements were mapped for all specimens (see for example Figs. 7 and 8). The out-of-roundness $A_0$ was then computed by Holt's method (Ref. 22, or method (d) of Ref. 23, or method (c) of Ref. 24). $A_0$ is given in Table 5.

As the pressure is increased gradually in the test, the Statham pressure gage is recalibrated against the mercury or alcohol head. The actual buckling pressures are, however, read on the potentiometer activated by the more sensitive Statham gage, and translated into pressure with the aid of the new calibration curve obtained during the test.

Three values of buckling pressure are recorded in each test: (1) The onset of buckling, (2) complete buckling, and (3) plastic collapse. The onset of buckling is the formation of the first true buckling wave, as distinct from the initial waviness which increases gradually with increase in pressure. This gradual increase in initial waviness is an equilibrium phenomenon, which only near

the critical load transforms into an instability phenomenon (usually with a "puck"). The onset of buckling is indicated by a loud "puck", accompanied by a small pressure drop.

The transition, with slow increase in pressure, from the first wave to the fully buckled condition is either gradual, the waves appearing one after the other (or in pairs) along the circumference each with a "puck", or it is sudden, the waves appearing along the entire circumference simultaneously with a large "puck". In many of the "good" specimens, with small out-of-roundness, the onset of buckling brought out all the lobes and represented therefore also complete buckling.

After the shell is fully buckled, the pressure is released and the test repeated, unless considerable plastic deformations are observed. In the second series (Alclad specimens), after two or three repetitons of the test, the upper end fixture is tightened to obtain partial clamping, and the test is repeated with the changed boundary conditions.

All the tests are continued into the plastic regime, and finally the plastic collapse pressure is recorded.

Since the standard tolerances for the thin gage sheet, of which the cones were made, permit thickness variations of up to ± 10% in a batch of the same nominal size, the thickness of the cones was again accurately measured. Thickness measurements were taken at 25 points for each specimen and averaged. The results indicated very small variations (of the order of – 0.01 – 0.02 mm) in the thickness of each specimen, but slightly larger variations of thickness between specimens (up to ± 0.03 mm). Hence for some specimens the nominal thickness had to be corrected accordingly.

## TEST SPECIMENS

In order to extend the range of geometrical parameters covered, the taper ratios of the specimens of the present tests were chosen to differ from those of Ref. 17. The geometries and the numbering of the specimens are summarized in Table 3. It should be noted, that the external pressure tests do not cover all the geometries given in the table, since some were tested only in torsion or under combined loading of torsion and external pressure (see Section 3).

TABLE 3
Geometries and Numbering of Specimens

| $\alpha_{(deg)}$ | $1/\rho_{av}$ | $H_{(mm)}$ | $R_{1\ (mm)}$ ** | Taper Ratio $\psi = 1-(R_1/R_2)$ | Serial Numbers | | | |
|---|---|---|---|---|---|---|---|---|
| | | | | | Stainless Steel Z 10CNT18 (* AG5 – X 516 Aluminum Alloy | | | |
| 30 | 2.52 | 463 | 50 | 0.843 | 311 | | 313 | |
| | 1.49 | 330 | 127 | 0.600 | | 317 | | 319* |
| 40 | 1.74 | 319 | 50 | 0.843 | 411 | | 413 | 414* |
| | 1.02 | 227 | 127 | 0.600 | 416 | 417 | | 419* |
| Alclad 2024–T3 | | | | | | | | |
| 30 | 2.52 | 463 | 50 | 0.843 | 321 | | | |
| | 1.49 | 330 | 127 | 0.600 | | 327 | 328 | |
| 40 | 1.74 | 319 | 50 | 0.843 | 421 | 422 | | |
| | 1.02 | 227 | 127 | 0.600 | 426 | | | |
| **For all specimens $R_2$ = 317.5 mm. | | | | Nominal $h_{(mm)}$ Thickness | 0.4 | 0.6 | 0.8 | 1.0 |

The test cones of the first series were made of annealed stainless steel Z 10 CNT 18 (a French specification of a non-heat-treatable stainless steel similar to the American 18-8 – 321). Some of the specimens of this series were made of a weldable aluminum alloy AG5 – X 516 (a French specification roughly similar to the American 5052). The specimens of the second series were made of 2024–T3 Alclad. The typical properties of these materials are given in Table 4.

TABLE 4
Mechanical Properties of Materials

| Material | Stainless Steel | Aluminum Alloy | Alclad |
|---|---|---|---|
| Specification | Z 10 CNT 18 | AG5 - X 516 | 2024 – T3 |
| E (psi) | $27.0 \times 10^6$ | $10.3 \times 10^6$ | $10.6 \times 10^6$ |
| $\nu$ | 0.3 | 0.3 | 0.33 |
| $\sigma_{yield\ (psi)}$ | 33000 | 20600 | 39000 |
| $\sigma_{UTS\ (psi)}$ | 78000 | 43000 | 59000 |

Typical specimens are shown in Figs. 9 and 10. As in the earlier investigations (Ref. 17), the specimens are fairly large, and were made by standard aircraft methods (described in Ref. 17) at the Israel Aviation Industries, Lod. For the first series of cones, butt-welded joints were employed in the aim to approach uniform shells as far as possible, and the type of steel was chosen on account of its excellent weldability. Argon welding was employed, and extreme care resulted in very uniform welds. However, some slight waviness still remained near the weld, nearly of the same order as occurred in the earlier aluminum alloy specimens (of Ref. 17). Though the measured initial out-of-roundness was not worse, and usually even better, than for the tests of Ref. 17, the initial test results for the steel cones were on the average much below those for the aluminum alloy specimens of the earlier investigations. Residual welding stresses were suspected to be the main cause of this reduction. Hence though the annealed Z 10 CNT 18 is basically non-heat treatable, stress relief heat-treatment to 550°C, and at a later stage to 990°C, was attempted, but without success, as can be seen from Table 5. Unrelated tests on the same material carried out at the same time by the metallurgical department of the Israel Aviation Industries, showed later that effective stress relief can be obtained only when the residual stresses are near the yield stress of the steel.

Theoretical results on the marked inferiority of stringers as stiffeners for cylindrical shells against general instability under external pressure (Ref. 25), initiated a review of the earlier dismissal of lap joints on account of their local stiffening effect. Since fairly strong stringers, distributed evenly around the circumference of a shell, were found to have raised the critical pressure only by a few percent, it was concluded that for buckling under external pressure the stiffening of a lap joint is entirely negligible. The second series of specimens was therefore made with an adhesive bonded lap joint. In the absence of weldability restrictions, a material with a relatively high yield stress, as appropriate for elastic buckling tests, could be chosen. Alclad 2024–T3 was used, and the shells were joined by an Epon-Versamid bond, with a very thin fibre-glass inter-surface mat to improve adhesion.

## RESULTS AND BUCKLING BEHAVIOUR

The geometry of the conical shells, the test results and the corresponding theoretical estimates

are given in Tables 5 and 6. The geometrical data includes also the initial out-of-roundness $\Delta_0$, measured after the specimen has been secured in the end fixtures, and for convenience the thickness is given also in inches. As in Ref. 17, the measured pressures at onset of buckling $p_0$, when the shell is fully buckled $p_f$, and at complete plastic collapse $p_p$ are given; and for comparison the theoretical values obtained by the methods of Niordson (Ref. 26), Seide (Ref. 18) and Singer (Ref. 1), follow. As discussed in Ref. 1, though different boundary conditions are assumed in the analyses of Refs. 1 and 18, their results differ only slightly.

The buckling behaviour of the two series of tests is basically similar. One noticeable difference is the practically instantaneous transition of the elastic buckling waves to plastic deformation, which is caused by the lower yield stress of the steel (and AG5 aluminum alloy) cones; or more precisely, by their higher ratios of elastic buckling stress to yield stress. For specimens which are perfect, the maximum theoretical buckling stress varies between 5.3% to 17.8% of the yield stress for the first series, whereas for the 2024–T3 Alclad specimens of the second series the theoretical critical stress is only between 1.7% to 6.3% of the yield stress. Hence, even without initial imperfections, not very large amplitudes of buckling waves are necessary in the thicker shells to reach the yield stress, though the buckling phenomenon itself was entirely elastic. Indeed, only when the buckling stress was a very small fraction of the yield stress, as in the case of the thinnest 2024 – T3 Alclad shells (Specimens 321 and 421, for which the maximum theoretical $\sigma_{crit.}$ is 1.7% and 2.1% respectively of $\sigma_{yield}$) could the pressure be arrested in time to ensure entirely elastic behaviour. The tests for these specimens could be repeated consistently a number of times on the same cone (see Table 6), while even for the thinnest steel cones consistent repetition was difficult (though occasionally very nearly achieved, for example with specimen 416/1).

The buckling behaviour of all the shells can be broadly divided into two groups: one, usually shells having pronounced local initial dimples, in which the pressure had to be increased considerably after onset of buckling to bring the shell to the fully buckled state; and one, consisting mainly of shells having small out-of-roundness, in which the maximum buckling pressure was reached already at the onset of buckling, coinciding sometimes actually with the fully buckled state, or developing then into the fully buckled state at a lower pressure. The complete plastic collapse, characterized by the

# TABLE 5

## BUCKLING OF STAINLESS STEEL CONES UNDER HYDROSTATIC PRESSURE

Test Data and Comparison with Theory († Cones made of AG 5 – X 516 aluminium alloy)

| | Specimen No. | $1-\frac{R_1}{R_2}$ | Thickness h | | $\rho_{av}/h$ | $l/\rho_{av}$ | $A_0$ | Measured Buckling Pressure $p_{cr}$ | | | $p_{cr}$ Theory (psi) | | | $p_0/p_{th_1}$ | $p_b/p_{th_1}$ | Number of Waves | |
|---|---|---|---|---|---|---|---|---|---|---|---|---|---|---|---|---|---|
| | | | mm | inches | | | mm | Onset of Buckling $p_0$ | Fully Buckled $p_f$ | Complete Plastic Collapse $p_p$ | Singer $p_{th_1}$ | Seide $p_{th_2}$ | Niordson $p_{th_3}$ | | | $n_e$ Experimental | $n_{th}$ Theory (Seide) |
| 90° | 311/1 □ | 0.843 | 0.4 | 0.0157 | 530 | 2.521 | 1.3 | 1.46 | 1.70 | 1.94 | 1.88 | 1.85 | 1.52 | 0.78 | 0.91 | 8 | 10 – 11 |
| | 311/2 • | 0.843 | 0.4 | 0.0157 | 530 | 2.521 | 1.1 | 1.41 | 1.47 | 2.02 | 1.88 | 1.85 | 1.52 | 0.75 | 0.78 | 9 | 10 – 11 |
| | 311/3 • | 0.843 | 0.4 | 0.0157 | 530 | 2.521 | 1.7 | 1.35 | 1.67 | 1.89 | 1.88 | 1.85 | 1.52 | 0.72 | 0.89 | 9 | 10 – 11 |
| | 311/7 ▲• | 0.843 | 0.4 | 0.0157 | 530 | 2.521 | 1.1 | 1.36 | 1.91 | 2.05 | 1.88 | 1.85 | 1.52 | 0.72 | 0.96 | 7 | 10 – 11 |
| | 311/8 ▲• | 0.843 | 0.4 | 0.0157 | 530 | 2.521 | 0.8 | 1.10 | 1.58 | 2.15 | 1.88 | 1.85 | 1.52 | 0.59 | 0.84 | 8 | 10 – 11 |
| | 311/9 • | 0.843 | 0.4 | 0.0157 | 530 | 2.521 | 1.1 | 1.24 | 1.45 | 2.03 | 1.88 | 1.85 | 1.52 | 0.66 | 0.77 | 8 | 10 – 11 |
| | 311/10 □ | 0.843 | 0.4 | 0.0157 | 530 | 2.521 | 1.0 | 1.26 | 1.36 | 1.94 | 1.88 | 1.85 | 1.52 | 0.67 | 0.72 | 7 | 10 – 11 |
| | 311/11 ▲ | 0.843 | 0.4 | 0.0157 | 530 | 2.521 | 3.1 | 1.18 | 1.44 | 1.96 | 1.88 | 1.85 | 1.52 | 0.63 | 0.77 | 7 | 10 – 11 |
| | 311/12 ▲ | 0.843 | 0.4 | 0.0157 | 530 | 2.521 | 0.5 | 1.35 | 1.31 | 2.14 | 1.88 | 1.85 | 1.52 | 0.72 | 0.72 | 8 | 10 – 11 |
| | 311/13 ▲ | 0.843 | 0.4 | 0.0157 | 530 | 2.521 | 0.8 | 1.21 | 1.38 | 2.14 | 1.88 | 1.85 | 1.52 | 0.64 | 0.73 | 7 | 10 – 11 |
| | 311/14 | 0.843 | 0.4 | 0.0157 | 530 | 2.521 | 1.2 | 1.015 | 1.24 | 1.76 | 1.88 | 1.85 | 1.52 | 0.54 | 0.66 | 6 | 10 – 11 |
| | 313/1 □ | 0.843 | 0.8 | 0.0315 | 265 | 2.521 | 2.1 | 7.90 | 9.41 | 9.65 | 10.63 | 10.47 | 8.58 | 0.74 | 0.89 | 8 | 9 |
| | 317/8 • | 0.600 | 0.6 | 0.0236 | 427 | 1.485 | 0.85 | 3.46 | 3.55 | 5.02 | 5.06 | 4.98 | 4.08 | 0.685 | 0.70 | 7 | 9 |
| 40° | 411/1 □ | 0.843 | 0.4 | 0.0157 | 600 | 1.735 | 0.5 | 1.22 | 1.34 | 2.2[illegible] | 2.01 | 1.98 | 1.62 | 0.61 | 0.67 | 7 | 10 – 11 |
| | 411/3 □ | 0.843 | 0.4 | 0.0157 | 600 | 1.735 | 1.1 | 1.33 | 1.68 | 2.30 | 2.01 | 1.98 | 1.62 | 0.66 | 0.84 | 7 | 10 – 11 |
| | 413/1 • | 0.843 | 0.8 | 0.0315 | 300 | 1.735 | 1.0 | 6.50 | 7.10 | 9.04 | 11.38 | 11.19 | 9.18 | 0.57 | 0.62 | 6 | 9 – 10 |
| | † 414/1 • | 0.843 | 1.02 | 0.0402 | 245 | 1.735 | 0.8 | 5.24 | 5.80 | 7.87 | 8.05 | 7.92 | 6.49 | 0.65 | 0.72 | 6 | 9 |
| | † 414/2 □ | 0.843 | 1.02 | 0.0402 | 245 | 1.735 | 0.5 | 6.01 | 6.18 | 7.95 | 8.05 | 7.92 | 6.49 | 0.75 | 0.77 | 6 | 9 |
| | 416/1 ▲• | 0.600 | 0.4 | 0.0157 | 725 | 1.023 | 0.9 | 1.26 | 1.66 | 2.92 | 1.93 | 1.93 | 1.71 | 0.65 | 0.86 | 10 | 10 |
| | 416/2 ▲• | 0.600 | 0.4 | 0.0157 | 725 | 1.023 | 0.6 | 1.53 | 1.61 | 2.90 | 1.93 | 1.93 | 1.71 | 0.79 | 0.83 | 9 | 10 |
| | 419/1 • | 0.600 | 1.0 | 0.0394 | 290 | 1.023 | 0.2 | 13.90 | 13.90 | 15.2 | 20.98 | 20.64 | 16.92 | 0.66 | 0.66 | 7 | 8 |
| | 419/2 • | 0.600 | 1.02 | 0.0402 | 296 | 1.023 | 0.5 | 12.75 | 12.75 | 15.4 | 22.05 | 21.69 | 17.78 | 0.58 | 0.58 | 7 | 8 |

• Buckling commenced near welded joint.

o Buckling commenced opposite welded joint.

▲ Stress-relief attempted

• All waves appeared simultaneously

# TABLE 6

## BUCKLING OF ALCLAD CONES UNDER HYDROSTATIC PRESSURE. DATA AND COMPARISON WITH THEORY.

(I, II, etc. repeated tests on same specimen)

| | Specimen No. | $1-\frac{R_1}{R_2}$ | Thickness h | | $\rho_{av}/h$ | $l/\rho_{av}$ | $A_0$ | Measured Buckling Pressure $p_{cr}$ | | | $p_{cr}$ Theory (psi) | | | $P_0/P_{th_1}$ | $P_b/P_{th_1}$ | Number of Waves | |
|---|---|---|---|---|---|---|---|---|---|---|---|---|---|---|---|---|---|
| | | | mm | inches | | | mm | Onset of Buckling $P_0$ | Fully Buckled $P_f$ | Complete Plastic Collapse $P_p$ | Singer $P_{th_1}$ | Seide $P_{th_2}$ | Niordson $P_{th_3}$ | | | $n_e$ Experimental | $n_{th}$ Theory (Seide) |
| $\alpha=40°$ | 421/1/I ▲ | 0.843 | 0.4 | 0.0157 | 600 | 1.730 | 0.3 | 0.655 | 0.655 | | | | | 0.830 | 0.830 | 8 | |
| | 421/1/II ▲ | 0.843 | 0.4 | 0.0157 | 600 | 1.730 | 0.3 | 0.645 | 0.645 | | 0.790 | 0.777 | 0.637 | 0.818 | 0.818 | 7 | 10 – 11 |
| | 421/1/III ▲ | 0.843 | 0.4 | 0.0157 | 600 | 1.730 | 0.3 | 0.572 | 0.572 | | | | | 0.724 | 0.736 | 7 | |
| | *421/1/IV | 0.843 | 0.4 | 0.0157 | 600 | 1.730 | 0.3 | 0.607 | 0.704 | 1.41 | | | | 0.770 | 0.890 | 7 | |
| | 421/2/I ▲ | 0.843 | 0.4 | 0.0157 | 600 | 1.730 | 0.2 | 0.694 | 0.694 | | | | | 0.878 | 0.878 | 7 | |
| | 421/2/II ▲ | 0.843 | 0.4 | 0.0157 | 600 | 1.730 | 0.2 | 0.680 | 0.680 | | 0.790 | 0.777 | 0.637 | 0.860 | 0.860 | 7 | 10 – 11 |
| | 421/2/III ▲ | 0.843 | 0.4 | 0.0157 | 600 | 1.730 | 0.2 | 0.669 | 0.669 | | | | | 0.846 | 0.846 | 7 | |
| | *421/2/IV ▲ | 0.843 | 0.4 | 0.0157 | 600 | 1.730 | 0.2 | 0.865 | 0.865 | 1.47 | | | | 1.095 | 1.095 | 7 | |
| | 421/3/I | 0.843 | 0.4 | 0.0157 | 600 | 1.730 | 0.6 | 0.590 | 0.590 | | | | | 0.746 | 0.746 | 8 | |
| | 421/3/II | 0.843 | 0.4 | 0.0157 | 600 | 1.730 | 0.6 | 0.587 | 0.590 | | 0.790 | 0.777 | 0.637 | 0.743 | 0.746 | 8 | 10 – 11 |
| | 421/3/III | 0.843 | 0.4 | 0.0157 | 600 | 1.730 | 0.6 | 0.575 | 0.575 | | | | | 0.728 | 0.728 | 8 | |
| | *421/3/IV | 0.843 | 0.4 | 0.0157 | 600 | 1.730 | 0.6 | 0.367 | 0.690 | 1.56 | | | | 0.465 | 0.874 | 9 | |
| | 421/4/I ▲ | 0.843 | 0.4 | 0.0157 | 600 | 1.730 | 0.2 | 0.677 | 0.677 | | | | | 0.856 | 0.856 | 8 | |
| | 421/4/II ▲ | 0.843 | 0.4 | 0.0157 | 600 | 1.730 | 0.2 | 0.703 | 0.703 | | 0.790 | 0.777 | 0.637 | 0.890 | 0.890 | 7 | 10 – 11 |
| | 421/4/III ▲ | 0.843 | 0.4 | 0.0157 | 600 | 1.730 | 0.2 | 0.694 | 0.694 | | | | | 0.878 | 0.878 | 7 | |
| | *421/4/IV | 0.843 | 0.4 | 0.0157 | 600 | 1.730 | 0.2 | 0.557 | 0.831 | 1.54 | | | | 0.705 | 1.050 | 8 | |
| | 421/5/I ▲ | 0.843 | 0.4 | 0.0157 | 600 | 1.730 | 0.1 | 0.704 | 0.704 | | | | | 0.890 | 0.890 | 9 | |
| | 421/5/II ▲ | 0.843 | 0.4 | 0.0157 | 600 | 1.730 | 0.1 | 0.696 | 0.696 | | 0.790 | 0.777 | 0.637 | 0.881 | 0.881 | 8 | 10 – 11 |
| | 421/5/III ▲ | 0.843 | 0.4 | 0.0157 | 600 | 1.730 | 0.1 | 0.688 | 0.688 | | | | | 0.871 | 0.871 | 8 | |
| | *421/5/IV ▲ | 0.843 | 0.4 | 0.0157 | 600 | 1.730 | 0.1 | 0.835 | 0.835 | 1.55 | | | | 1.057 | 1.057 | 9 | |
| | 421/6/I ▲ | 0.843 | 0.4 | 0.0157 | 600 | 1.730 | 0.2 | 0.707 | 0.707 | | | | | 0.895 | 0.895 | 7 | |
| | 421/6/II ▲ | 0.843 | 0.4 | 0.0157 | 600 | 1.730 | 0.2 | 0.703 | 0.703 | | 0.790 | 0.777 | 0.637 | 0.890 | 0.890 | 7 | 10 – 11 |
| | 421/6/III ▲ | 0.843 | 0.4 | 0.0157 | 600 | 1.730 | 0.2 | 0.718 | 0.718 | | | | | 0.909 | 0.909 | 7 | |
| | *421/6/IV ▲ | 0.843 | 0.4 | 0.0157 | 600 | 1.730 | 0.2 | 0.790 | 0.790 | 1.50 | | | | 1.000 | 1.000 | 9 | |
| | 421/7/I ▲ | 0.843 | 0.4 | 0.0157 | 600 | 1.730 | 0.35 | 0.635 | 0.635 | | | | | 0.804 | 0.804 | 8 | |
| | 421/7/II ▲ | 0.843 | 0.4 | 0.0157 | 600 | 1.730 | 0.35 | 0.650 | 0.650 | | 0.790 | 0.777 | 0.637 | 0.823 | 0.823 | 8 | 10 – 11 |
| | 427/III ▲ | 0.843 | 0.4 | 0.0157 | 600 | 1.730 | 0.35 | 0.653 | 0.653 | | | | | 0.827 | 0.827 | 8 | |
| $\alpha=30°$ | 321/3/I | 0.843 | 0.4 | 0.0157 | 530 | 2.521 | 0.50 | 0.505 | 0.505 | | | | | 0.665 | 0.665 | 7 | |
| | 321/3/II | 0.843 | 0.4 | 0.0157 | 530 | 2.521 | 0.50 | 0.514 | 0.514 | | 0.758 | 0.745 | 0.611 | 0.677 | 0.677 | 7 | 9 – 10 |
| | 321/3/III | 0.843 | 0.4 | 0.0157 | 530 | 2.521 | 0.50 | 0.507 | 0.514 | | | | | 0.667 | 0.677 | 7 | |
| | *321/3/IV | 0.843 | 0.4 | 0.0157 | 530 | 2.521 | 0.50 | 0.560 | 0.660 | 1.205 | | | | 0.738 | 0.870 | 8 | |
| | 321/4 † | 0.843 | 0.4 | 0.0157 | 530 | 2.521 | 1.10 | 0.46 | 0.483 | | 0.758 | 0.745 | 0.611 | 0.606 | 0.637 | 8 | 9 – 10 |
| | 327/1 ▲ | 0.600 | 0.63 | 0.0251 | 407 | 1.489 | 0.55 | 1.96 | 1.96 | 3.85 | 2.60 | 2.562 | 2.10 | 0.753 | 0.753 | 7 | 9 |
| | 328/1 ▲ | 0.600 | 0.80 | 0.0315 | 320 | 1.489 | 0.60 | 3.91 | 3.91 | 6.39 | 4.87 | 4.80 | 3.93 | 0.815 | 0.815 | 7 | 8 |

• Clamped

▲ Onset of buckling $p_0$ and complete buckling $p_f$ simultaneously

† Buckling commences locally at initial dimples (see Fig. 8)

typical "folding" of buckles (see Figs. 12 and 14) and accompanied by a large pressure drop, occurred finally in both groups always at a much higher pressure.

As in Ref. 17, the buckling pressure from the point of view of the designer (as emphasized by Hoff, Ref. 27), being the maximum pressure which the shell can carry without noticeable plastic deformation, is considered. Here, this is the pressure when the shell is fully buckled $p_f$ (see Figs. 11 and 13), or the pressure at the onset of buckling $p_0$, whichever is greater, and it is designated here the buckling pressure $p_b$. Though it may seem logical to compare the critical pressure, obtained by the small deflection analyses of Refs. 1, 18 or 26 with the experimental values for onset of buckling, it was found in Ref. 17 that the onset of buckling is too sensitive to initial imperfections of the specimen to be a useful criterion. In Tables 5 and 6, $p_0/p_{th}$ is also given, but the comparison of $p_b$ with theory is a better indication of the reliability of the theory. Hence in Figs. 14 – 16, $p_b$ is presented.

As far as can be judged from the reports (Refs. 19 to 21, 28), most previous experimental investigations also recorded $p_b$ and not $p_0$. For example, Magula (Ref. 28) calls $p_b = p_f$ the "initial buckling pressure", while in one of his tests the first wave appeared at a $p_0$, being 33% lower, which is not considered. It may also be noted, that recent experimental work on cylindrical shells (see for example Ref. 29) also records buckling loads in the sense defined above and not the onset of buckling.

In Figs. 14 to 16 the ratio of buckling pressure $p_b$ to the critical pressure of an equivalent cylindrical shell, of length $l$ (the slant length of the cone) radius $\rho_{av}$ (the mean radius of curvature of the cone) and the same thickness $h$, $p_{th_3}$, is plotted versus the taper ratio $\psi = 1-(R_1/R_2)$, $p_{th_3}$ is essentially that computed by Niordson's method (Ref. 26), except that the critical pressure for the equivalent cylindrical shell arrived at by the Niordson's analysis is obtained instead of by von Mises's formula (Ref. 30), by a very close approximation to it, as discussed in Refs. 17 or 18.

The first series of tests is summarized in Table 5 and Fig. 14. If one compares Fig. 14 with Fig. 11 of Ref. 17, it is immediately apparent that the results are rather low. The mean of the experimental points falls for both taper ratios about 20% below the theoretical curve. A possible cause for the consistent poor results would be residual welding stresses, if compressive stresses of the order of 20% of the theoretical buckling were found. Tests were carried out on two typical steel shells (311/14 and 411/4). 22 and 20 strain gages, respectively, were attached to the rolled shell prior to welding (at each location, one on each side of the sheet, and both connected in series so as to measure only mem-

brane stresses), and balanced. The shell was then welded in exactly the same manner as the regular specimens, and finally after completion, the change in strain was recorded. Circumferential residual strains of 20 – 30 $\mu$ in./in. were recorded, which correspond to residual circumferential stresses of 500 to 800 psi. Compressive and tensile stresses appear, which vary and change signs rapidly along a generator (due to the method of welding, in which a considerable number of tack welds preceeded the continuous seam), but exhibit only slow changes along the circumference. More extensive testing and strain gaging would be required to give good quantitative estimates of the welding stresses, but the tests demonstrated very clearly the presence of residual compressive circumferential stresses of up to 25% and even 45% of the maximum critical buckling stress under external pressure, whose mean effect may reduce the critical pressures by 15% to 25%, as observed. A similar test on an AG 5 aluminum alloy specimen of double thickness (413) revealed similar magnitudes of residual strains, which however correspond to stresses that are less than 15% of the critical stresses. Smaller reductions in critical pressures of 5% to 10% should therefore result. These residual welding stresses appear, however, to be also an important factor in the interpretation of the test results obtained with butt-welded aluminum alloy cones (Ref. 17).

As a further check on the cause of the low results for the steel cones (Fig. 15), strain gages were attached to one specimen (311/14), and the theoretical buckling pressure which would appear for a perfect conical shell was determined from the strain gage readings by the extension of Southwell's method given for cylindrical shells in Ref. 31. The slope method suggested there was used, and yielded a perfect cone buckling pressure of about 1.29 psi, 31% below the theoretical critical pressure. Since even after the elimination of the effect of initial imperfections, a very low result is obtained, the residual welding stresses appear indeed to be the prime cause of the reduced buckling pressures.

Hence, the welded steel specimens should not be relied upon for evaluation of the theory, unless one reduces the theoretical curve by about 20% on account of the existing prestress state, as is shown by the dotted line in Fig. 15. The points of Fig. 15 are therefore not included in Fig. 17, which compares various experimental results with theory.

The second series of bonded 2024 – T3 Alclad specimens yielded much better results, as can be seen in Table 6 and Fig. 16 (the mean of the repeated tests are presented in the figure). These

tests revealed that the end conditions are of much greater importance for thin shells under external pressure than is usually assumed. In most buckling experiments of cylindrical or conical shells the end fixtures represent practically clamped ends, but the test results are compared with theories for simple supports, based on the argument that due to the low bending stiffness of a thin shell the effect of the boundary conditions on the buckling process is negligible. (For example, Ref. 19, 29, 35, 36). Galletly, Slankard and Wenk (Ref. 36) tried to attain fully clamped boundary conditions but obtained very good agreement with theories for simple supports. In the present tests the end fixtures were designed to approach simple supports as far as possible; however, by tightening the bolts connecting the end rings very much, partial clamping was achieved. This was done for 7 thin Alclad specimens (421 and 321) for which repeated tests were easily carried out. In these tests the specimen was first attached with simple supports, by minimum tightening of top and fixture bolts (tightening by fingers only), and tested to the fully buckled state, and retested a number of times. Then the top end fixture bolts were tightened appreciably and the test repeated with the top end partially clamped (seeTable 6).

The Alclad specimens had in general much lower out-of-roundness, and the onset of buckling and complete buckling occurred simultaneously. The repeated tests of the same specimens, with simple supports, resulted in only a small scatter of the results (about 5%). The simple support behaviour of the end fixtures was verified by the observed transfer of the slope of the buckling waves beyond the fixture to the overlap of the cones.

The partial clamping of the top end, in the last part of each test, resulted in a mean increase of 18% in the buckling pressure. This demonstrates very clearly the importance of the boundary conditions in the buckling process of conical shells under external pressure, even for very thin shells. Since the tightening of the end fixture bolts was not kept under careful control during the tests of Ref. 17, this may be one of the causes of the scatter of the results there.

The tests of the Alclad specimens reconfirm with more certainty the conclusions of Ref. 17 about the validity of the theories of Singer (Ref. 1) and Seide (Ref. 18). This is shown in Fig. 17 in which the present results (except the steel cones of Table 5) are compared with those of Ref. 17, other tests and theories. The theories are verified to the same extent as the classical linear theory for cylindrical shells (Ref. 30). The older experiments which verified that theory so neatly (see, for example, Fig. 6 of Ref. 7) were for cylinders of small (R/h) ratios. More recent tests with much higher (R/h) ratios

show a scatter of the same order as Fig. 17,(see Ref. 37, or Ref. 19).

The conclusions of Ref. 17 about the effect of the initial out-of-roundness, are reconfirmed here. Since the critical stresses are very far from the yield stress, even for the steel specimen, and the specimens have medium or high $(\rho_{av}/h)$ ratios, the published results on cylindrical shells (Refs. 32 – 34), which are for very short shells of low (R/h) ratios, could not be applied. Examination of the pre-test circularity contours (see for example Figs. 7 and 8), and their corresponding buckling behaviour, as in Ref. 17, yielding similar observations, though for the thin, and fairly accurate, Alclad specimens the out-of-roundness was found to have a more pronounced effect on the buckling pressure (for example, shell 321/4 – see Table 6 and Fig. 16).

In Fig. 18 the plastic collapse pressures are plotted together with those obtained in Ref. 17. The parametric form of Ref. 17 $(h/\rho_{av})\, C_{p_p}$ versus $\bar{Z}$ is used,

where the non-dimensional parameters are

$$\bar{Z} = (l/\rho_{av})^2 (1 - \nu^2)^{\frac{1}{2}} \tag{2.1}$$

and

$$C_{p_p} = [12 (1 - \nu^2)/\pi^2] (p_p/E) (l/h)^2 (\rho_{av}/h) \tag{2.2}$$

The steel cones of Table 5 are again not included, since also their plastic collapse pressures were much below all others. This fact presents another indirect proof of the presence of the residual stresses discussed above.

The averaging empirical formula of Ref. 17.

$$C_{p_p} = (\rho_{av}/h)\, 0.090\, \bar{Z}^{0.42} \tag{2.3}$$

appears to apply also to the present results of Table 6, though it is slightly conservative.

# SECTION 3

## EXPERIMENTAL INVESTIGATION OF THE BUCKLING OF CONICAL SHELLS UNDER COMBINED TORSION AND EXTERNAL PRESSURE

Josef Singer

# INTRODUCTION

Until very recently, no experimental data was available on the buckling of conical shells under torsion except a few tests by Lundquist and Schuette on truncated cones having a cone angle of 11 degrees (Ref. 38). At Space Technology Laboratories (Ref. 19) a series of preliminary tests on steel cones in torsion were recently carried out. These tests covered a $(\rho_{av}/h)$ range of 867 – 1500, with cone angles of 30° and 60°. The purpose of the present torsion tests was to provide more experimental data for verification of the theory of Seide (Ref. 10) and of the present report, to extend the range of geometries, and to provide reference points for the tests under combined torsion and external pressure, which formed the main purpose of the program. The torsion tests covered a $(\rho_{av}/h)$ range of 320 – 725, with cone angles of 30° and 40°. The combined torsion and external pressure test covered a $(\rho_{av}/h)$ range of 256 – 725, again with cone angles of 30° and 40°. 41 specimens were tested in the program reported in this section. Part of the specimens were made of annealed stainless steel Z 10 CNT 18, and the remainder of 2024 – T3 Alclad. The geometries are given in Table 3.

# TEST APPARATUS AND PROCEDURE

The test rig for the experimental program of buckling under torsion and under combined torsion and external pressure is shown in Figs. 4 & 5. It is an adaption of the pressure vessel used in previous tests. The conical shells are mounted as in the previous tests, but in order to ensure that the applied load is pure torsion, the cone and torque arm float in a central bearing anchored to the bottom of the vessel. Special care was taken during manufacture in centering this bearing with respect to the top flange. The torque arm, which is overdesigned for extra stiffness, rides in its main bearing, attached to the top flange, and the load is applied by a pair of jacks fed by a separate hydraulic system. The jacks are attached to the side frames and apply the load via strain-gage load beams (load cells) which are read continuously during the test.

As shown in Fig. 5 the end fittings are similar to those used in the earlier tests of Ref. 17, except that the inner rings are serrated to prevent slippage of the specimens. Also, for the cones with

small lower end radius, the outer lower ring was replaced by an aluminum ring which has a straight wedge profile, instead of the circular one with the O-seal, used otherwise. This end fixture caused more restraint, but was necessary to prevent slippage (note that a small radius results in very high shear loads). In general, the end fixture bolts had to be tightened much more in the torsion, and torsion plus external pressure tests, than previously. This removes the test conditions considerably from the assumed simple supports, but is still further from the clamped boundary conditions than, for example, the cast Cerrolow end attachment of Ref. 19.

The fitting and centering of specimens and the out-of-roundness measurements are similar to those described in Section 2 and in Ref. 17. There, an additional circularity contour was obtained near the small end of the cone, where the maximum shear stresses occur, and buckling commences. For torsion tests, the torque is applied by the jacks by means of an hydraulic pump. The jack pressure is recorded for reference, but the actual force applied by the jacks to the arm is measured by the precalibrated load beams which are read, via a switching and balancing unit, on an SR4 strain indicator. The angle of twist is measured with a light ray from a scale reflected with a mirror (which is attached to the axis of the cone) to a microscope. The torque is increased in small increments till buckling occurs. Buckling appears very clearly on the microscope, as a sudden "running" of the scale, or even a strong vibration of the image when the wave formation is very sudden and violent. Simultaneously, the SR4 indicator shows a sudden drop of torque, which is actually the most sensitive indication. "Puck"s cannot be entirely relied upon here, since especially for the cones of large taper ratio (small lower end radius), buckling occurs often "quietly", since it concentrates around the small end (see Fig. 19).

The tests under combined loading were carried out in two ways: (a) Going up to a predetermined pressure, and then keeping it constant while torque is applied till the shell buckles. (b) Similarly, only with torque instead of pressure being kept constant. The two procedures yielded fairly close results, the difference being smaller than the experimental scatter in general, which indicates that linear theory is applicable.

All the tests were continued beyond the point of buckling to obtain post-buckling curves (see for example Fig. 21). The Alclad specimens were retested a number of times, but though the twisting deformation disappeared entirely upon release of loads, the successive results were always slightly lower. This demonstrates the greater sensitivity of buckling in torsion to initial imperfections.

The tests were usually continued well into the region of plastic deformations.

## TORSION TESTS

The results of the pure torsion tests are given in Table 7, and are plotted and compared with theory in Fig. 22.

The buckling behaviour of conical shells of small taper ratio (see Fig. 20) is very similar to that of cylindrical shells. The waves cover most of the height of the cone and they resemble closely those of a cylinder also in form. For conical shells of large taper ratio, the buckling waves concentrate entirely near the small end (see Fig. 19), and their form differs.

In Fig. 22 the results of Table 7 are compared with theory. The critical torsion ratio, which is the experimental critical torque divided by $\bar{T}$, that of an equivalent cylinder for which

$$\begin{aligned} R &= \rho_{av} \\ L &= l \\ h &= h \end{aligned} \tag{3.1}$$

multiplied by $\cos^2 \alpha$. The curve plotted in Fig. 22 is based on Seide's theory (Ref. 10) and his points (Table 1 of Ref. 10). The corresponding values of the 3 typical shells computed in Section 1 of this report are also included and they are practically identical.

The comparison (of Table 7 and Fig. 22) shows good agreement with linear theory. The average discrepancy is 15%, with a maximum of 25%. The results are slightly closer to theory than the exploratory tests of Ref. 19, though the ends here were clamped to a lesser degree.

The results verify the linear theories of Ref. 10 and Section 1 of this report. It should be noted, however, that both theories are for simple supports, whereas in the tests, the ends were at least partly clamped and at the lower end the effect may be considerable.

The present tests seem to indicate that the design value of 75% of linear results given in Ref. 19 could be raised to 80% of the linear results. But more tests are required to determine the de-

# TABLE 7

## BUCKLING OF ALCLAD AND STEEL CONES IN TORSION

## TEST DATA AND COMPARISON WITH THEORY

| | Specimen No. | $\alpha°$ | $\psi$ Taper Ratio | Thickness h | | $\rho_{av}/h$ | $1/\rho_{av}$ | $A_0$ mm. | Maximum Critical Shear Stress [psi] | | | $\tau_e/\tau_{th_{Seide}}$ | $T/\bar{T}\cos^2\alpha$ | Number of Waves | |
|---|---|---|---|---|---|---|---|---|---|---|---|---|---|---|---|
| | | | | mm. | inch. | | | | Measured $\tau_{max_e}$ | Theoretical $\tau_{max}$ (Singer) | Theoretical $\tau_{max}$ (Seide) | | | $n_e$ Measured | $n_{th}$ Theoretical (Seide) |
| ALCLAD | 321 1 | 30° | 0.843 | 0.4 | 0.0157 | 530 | 2.521 | 0.35 | 13570 | – | 15320 | 0.885 | 0.516 | 7 | 8 |
| | 321/6 | 30° | 0.843 | 0.4 | 0.0157 | 530 | 2.521 | 0.45 | 13900 | – | 15320 | 0.907 | 0.526 | 7 | 8 |
| | 328/2 | 30° | 0.600 | 0.8 | 0.0315 | 320 | 1.286 | 0.25 | 11490 | – | 12630 | 0.908 | 0.722 | 10 | 10 |
| | 328/3 | 30° | 0.600 | 0.8 | 0.0315 | 320 | 1.286 | 0.7 | 11200 | – | 12630 | 0.888 | 0.705 | 10 | 10 |
| | 421/8 | 40° | 0.843 | 0.4 | 0.0157 | 600 | 1.732 | 0.4 | 12830 | 16320 | 16100 | 0.799 | 0.472 | 8 | 10 |
| | 421/13 | 40° | 0.843 | 0.4 | 0.0157 | 600 | 1.732 | 0.23 | 14090 | 16320 | 16100 | 0.875 | 0.520 | 8 | 10 |
| STEEL | 416/3 | 40° | 0.600 | 0.4 | 0.0157 | 725 | 1.021 | 0.8 | 10550 | 14150 | 14030 | 0.752 | 0.660 | – | 12 |
| | 416/4 | 40° | 0.600 | 0.4 | 0.0157 | 725 | 1.021 | 0.4 | 12300 | 14150 | 14030 | 0.877 | 0.770 | 10 | 12 |
| | 416/5 | 40° | 0.600 | 0.4 | 0.0157 | 725 | 1.021 | 0.85 | 10550 | 14150 | 14030 | 0.752 | 0.660 | 9 | 12 |

# TABLE 8

## BUCKLING UNDER COMBINED TORSION AND EXTERNAL PRESSURE

### TEST DATA

| $\alpha^c$ | Specimen No. | Material | $1-\frac{R_1}{R_2}$ | Thickness h | | $\rho_{av}/h$ | $l/\rho_{av}$ | $A_o$ mm. | Measured Pressure p [psi] | PRESSURE FOR ZERO TORQUE (Experimental or extrapolated from experimental data) $p_{T=0}$ (psi) | $p/p_{T=0}$ | Measured Maximum Shear Stress $\tau$ (psi) | MAX. SHEAR STRESS FOR ZERO PRESSURE (Experimental or extrapolated from experimental data) $\tau_{p=0}$ (psi) | $\tau/\tau_{p=0}$ | Number of Waves [Experimental] |
|---|---|---|---|---|---|---|---|---|---|---|---|---|---|---|---|
| | | | | mm. | inch. | | | | | | | | | | |
| 30° | 311/6 | Steel | 0.843 | 0.4 | 0.0157 | 530 | 2.521 | 0.5 | 1.50 | 1.58 | 0.950 | 12680 | 36400 | 0.348 | 9 |
| 30° | 317/1 | " | 0.600 | 0.6 | 0.0236 | 427 | 1.485 | 0.5 | 3.86 | 4.14 | 0.931 | 7500 | 15870 | 0.473 | 9 |
| 30° | 317/2 | " | 0.600 | 0.6 | 0.0236 | 427 | 1.485 | 0.7 | 3.22 | 4.14 | 0.778 | 3410 | 15870 | 0.215 | 8 |
| 30° | 317/3 | " | 0.600 | 0.6 | 0.0236 | 427 | 1.485 | 1.2 | 3.21 | 4.14 | 0.775 | 5020 | 15870 | 0.316 | 7 |
| 30° | 317/4 | " | 0.600 | 0.6 | 0.0236 | 427 | 1.485 | 1.15 | 2.89 | 4.14 | 0.698 | 7070 | 15870 | 0.445 | 8 |
| 30° | 317/5 | " | 0.600 | 0.6 | 0.0236 | 427 | 1.485 | 0.8 | 3.63 | 4.14 | 0.876 | 2750 | 15870 | 0.173 | 8 |
| 30° | 317/6 | " | 0.600 | 0.6 | 0.0236 | 427 | 1.485 | 1.3 | 3.21 | 4.14 | 0.775 | 4170 | 15870 | 0.262 | |
| 30° | 318/7 | " | 0.600 | 0.6 | 0.0236 | 427 | 1.485 | 1.4 | 2.59 | 4.14 | 0.625 | 7500 | 15870 | 0.473 | – |
| 30° | 319/1 | Al. Alloy | 0.600 | 1.00 | 0.0394 | 256 | 1.485 | 1.0 | 4.50 | 5.77 | 0.780 | 6650 | 14480 | 0.458 | 7 |
| 30° | 319/2 | " | 0.600 | 1.00 | 0.0394 | 256 | 1.485 | 0.7 | 4.78 | 5.77 | 0.830 | 3710 | 14480 | 0.256 | 7 |
| 30° | 319/3 | " | 0.600 | 1.00 | 0.0394 | 256 | 1.485 | 0.8 | 4.16 | 5.77 | 0.722 | 6860 | 14480 | 0.473 | 7 |
| 30° | 319/4 | " | 0.600 | 1.00 | 0.0394 | 256 | 1.485 | 0.45 | 5.07 | 5.77 | 0.880 | 6790 | 14480 | 0.469 | 7 |
| 30° | 319/5 | " | 0.600 | 1.00 | 0.0394 | 256 | 1.485 | 0.9 | 5.56 | 5.77 | 0.965 | 3270 | 14480 | 0.226 | 7 |
| 40° | 413/3 | Steel | 0.843 | 0.8 | 0.0315 | 300 | 1.735 | 0.6 | 4.89 | 8.54 | 0.572 | 30500 | 79000 | 0.386 | – |
| 40° | 413/4 | " | 0.843 | 0.8 | 0.0315 | 300 | 1.735 | 0.7 | 7.84 | 8.54 | 0.917 | 25780 | 79000 | 0.326 | – |
| 40° | 413/5 | " | 0.843 | 0.8 | 0.0315 | 300 | 1.735 | 0.7 | 7.08 | 8.54 | 0.826 | 31180 | 79000 | 0.395 | – |
| 40° | 416/6 | " | 0.600 | 0.4 | 0.0157 | 725 | 1.023 | 0.7 | 0.81 | 1.635 | 0.495 | 8290 | 11370 | 0.728 | 10 |
| 40° | 416/7 | " | 0.600 | 0.4 | 0.0157 | 725 | 1.023 | 0.95 | 0.82 | 1.635 | 0.501 | 7680 | 11370 | 0.675 | 9 |
| 40° | 416/8 | " | 0.600 | 0.4 | 0.0157 | 725 | 1.023 | 0.7 | 0.60 | 1.635 | 0.367 | 9620 | 11370 | 0.845 | 8 |
| 40° | 417/2 | " | 0.600 | 0.6 | 0.0236 | 483 | 1.023 | 0.45 | 4.02 | 4.60 | 0.874 | 2920 | 18860 | 0.154 | 9 |
| 40° | 417/3 | " | 0.600 | 0.6 | 0.0236 | 483 | 1.023 | 0.45 | 3.47 | 4.60 | 0.753 | 7890 | 18860 | 0.418 | 8 |
| 40° | 417/4 | " | 0.600 | 0.6 | 0.0236 | 483 | 1.023 | 0.8 | 3.19 | 4.60 | 0.692 | 7940 | 18860 | 0.421 | 8 |
| 40° | 417/6 | " | 0.600 | 0.6 | 0.0236 | 483 | 1.023 | 0.5 | 3.82 | 4.60 | 0.830 | 6910 | 18860 | 0.366 | 9 |
| 30° | 321/2 | Alclad | 0.843 | 0.4 | 0.0157 | 530 | 2.521 | 0.7 | 0.44 | 0.634 | 0.695 | 10690 | 13730 | 0.780 | 6 |
| 40° | 421/9 | " | 0.843 | 0.4 | 0.0157 | 600 | 1.735 | 0.15 | 0.36 | 0.671 | 0.537 | 12010 | 13440 | 0.894 | 8 |
| 40° | 421/10 | " | 0.843 | 0.4 | 0.0157 | 600 | 1.735 | 0.5 | 0.62 | 0.671 | 0.924 | 6590 | 13440 | 0.491 | 7 |
| 40° | 421/11 | " | 0.843 | 0.4 | 0.0157 | 600 | 1.735 | 0.3 | 0.52 | 0.671 | 0.775 | 5850 | 13440 | 0.436 | 8 |
| 40° | 421/12 | " | 0.843 | 0.4 | 0.0157 | 600 | 1.735 | 0.3 | 0.53 | 0.671 | 0.790 | 8130 | 13440 | 0.605 | 7 |
| 40° | 422/1 | " | 0.843 | 0.6 | 0.0236 | 400 | 1.735 | 0.7 | 1.58 | 1.85 | 0.853 | 11620 | 21080 | 0.552 | 6 |
| 40° | 422/3 | " | 0.843 | 0.6 | 0.0236 | 400 | 1.735 | 1.15 | 1.24 | 1.85 | 0.670 | 14010 | 21080 | 0.665 | 6 |
| 40° | 422/4 | " | 0.843 | 0.6 | 0.0236 | 400 | 1.735 | 0.9 | 1.32 | 1.85 | 0.714 | 11740 | 21080 | 0.558 | 6 |
| 40° | 422/5 | " | 0.843 | 0.6 | 0.0236 | 400 | 1.735 | 0.7 | 0.89 | 1.85 | 0.481 | 16940 | 21080 | 0.804 | 6 |

sign factor with more certainty. A further series of torsion tests is in preparation.

The experimentally determined number of waves agrees fairly well with the theoretical estimates (computed from the approximate curve of Ref. 10).

## COMBINED TORSION AND EXTERNAL PRESSURE

The results of the combined torsion and external pressure tests are given in Table 8,

Since the purpose of these tests was to verify the theoretical interaction curves of Section 1, and to provide data for empirical interaction curves, the measured pressures and maximum shear stresses (actually torque were measured) were not compared with the theoretical values, but with the mean of test results for pressure alone or torsion alone. In those cases where no appropriate experimental results were available, the existing results were extrapolated, in accordance with Seide's approximate formulae of Ref. 18 and 10, from the nearest experimental point.

The theoretical anal, showed that the interaction curves for large taper ratio and small or medium taper ratio differ considerably. The shells of taper ratio 0.843 are therefore plotted separately in Fig. 24, and compared with the interaction curve for shell 421 computed in Section 1; whereas those of taper ratio 0.600 are plotted in Fig. 25, and are compared there with the semi-empirical formula of Ref. 13. In Section 1 it was shown that for conical shell 416 (of medium taper ratio) the interaction curve can be approximated closely by this formula, Eq. (1.61).

The experimental results verify both interaction curves reasonably well, though with some scatter (more pronounced with the steel specimens). The different curve for the large taper ratio shells is emphasized by the results.

Hence, complete families of interaction curves for the entire range of conical shells of large taper ratio would be of value.

# SECTION 4

# BUCKLING OF CIRCULAR CONICAL SHELLS UNDER UNIFORM AXIAL COMPRESSION

Josef Singer

In Ref. 40 the axisymmetrical buckling of conical shells under axial compression was investigated. By setting Poisson's ration equal to zero (with the justification that buckling loads are usually not sensitive to Poisson's ratio), the buckling load was found to be

$$P_{cr} = P_{cyl\,\infty} \cos^2 \alpha = \{2\pi E h^2/[3(1-\nu^2)]^{\frac{1}{2}}\} \cos^2 \alpha \qquad ...(4.1)$$

In Ref. 41 the buckling under axial compression and external or internal uniform hydrostatic pressure was analysed without prescribing axisymmetry. For the case of axial compression and internal pressure the axisymmetrical buckling mode predominates, whereas for axial and external pressure the more general mode with many lobes along the circumference is critical. Buckling loads for axial compression only were not computed in this analysis on account of the very poor convergence of the stability determinant for zero external (or internal) pressure. For this case, the approximation of Eq. (4.1) was assumed to hold, since some spot calculations indicated it to be sufficiently accurate. Both Refs. 40 and 41 assume simple supports defined by the geometric (essential) boundary conditions

$$w \cos \alpha - u \sin \alpha = 0$$

$$v = 0 \qquad \text{at} \qquad x = 1, x_2 \qquad ...(4.2)$$

representing bulkheads which are rigid in a plane perpendicular to the axis and very flexible in the axial direction; whereas in this report the usual simple support conditions for conical shells are assumed, which are defined (as for cylindrical shells) by the geometric boundary conditions

$$w = 0$$

$$v = 0 \qquad \text{at} \qquad x = 1, x_2 \qquad ...(4.3)$$

and represent bulkheads which are rigid in the radial direction and very flexible in the direction of the generators. (Both definitions imply the natural boundary conditions of free rotation of generators about the edges, and freedom from restraint in the direction of the axis, or the generators, respectively).

The method of Ref. 1 is therefore extended and applied to the analysis of buckling under uniform axial compression. As mentioned in Section 1, this method of solution implies elastic restraints which approximate the condition of $v = 0$ very closely, and also the effect of the u restraint has been found to be practically negligible in the case of external pressure and torsion. In Ref. 42, the effect of axial constraint of the instability of circular cylindrical shells under uniform axial compression was shown to be even smaller than in the cases of external pressure loading, and hence its effect can also be neglected here.

The membrane stresses in the case of uniform axial compression are

$$\bar{\sigma}_x = -(P/2\pi h a x \sin\alpha \cos\alpha)$$

$$\bar{\sigma}_\phi = 0$$

$$\bar{\tau}_{x\phi} = 0 \qquad \ldots(4.4)$$

Now, assuming again that for the buckling analysis the prebuckling stress is represented satisfactorily by the membrane stresses, Eqs. (4.4), the modified third stability equation, Eq. (1.9), becomes

$$(1/x^2 \sin^2\alpha)\, H_2(w) + K^4 (P/E)(1/2\pi h a x \sin\alpha \cos\alpha)\, w_{,xx} + (1/x^3) K^4 \cos^2\alpha\, H_2^{-1}[(x^3 w_{,xx})_{,xx}] = 0 \qquad (4.5)$$

Substitution of the solution of Ref. 1 in Eq. (4.5), and evaluation by the Galerkin method as in Ref. 1, yields after some manipulations

$$\Sigma C_n S(n,m) = \Sigma C_n \{[(-1)^{m+n} x_2^{2\gamma-2} - 1] G_1(n,m) + K^4 \cos^2\alpha [(-1)^{m+n} x_2^{2\gamma} - 1] G_2(n,m) + \eta [(-1)^{m+n} x_2^{2\gamma-1} - 1] G_5(n,m) = 0 \qquad (4.6)$$

where $G_1(n,m)$ and $G_2(n,m)$ are again given by Eqs. [64] to [66] of Ref. 1 (which are repeated for

convenience in Appendix A)

$$G_5(n,m) = K_3(n)\left[\frac{m+n}{(2\gamma-1)^2+(m+n)^2\beta^2} + \frac{m-n}{(2\gamma-1)^2+(m-n)^2\beta^2}\right]$$

$$+ K_4(n)\left[\frac{1}{(2\gamma-1)^2+(m+n)^2\beta^2} - \frac{1}{(2\gamma-1)^2+(m-n)^2\beta^2}\right] \qquad (4.7)$$

$$K_3(n) = n\beta^2(2\gamma-1) \qquad (4.8)$$

$$K_4(n) = (2\gamma-1)[(\gamma^2-\gamma)-n^2\beta^2] \qquad (4.9)$$

and

$$\eta = (P/E)(K^4/2\pi h\, a \sin\alpha\cos\alpha) \qquad (4.10)$$

As in Ref. 1. N linear equations are obtained for an N term solution, and the lowest eigenvalue $\eta$ of the determinant of the coefficients of $C_n$ yields the buckling load. However, it should be noted that whereas in the case of buckling under external pressure (Ref. 1) $n = 1$ is always the basic mode (which consists of one half wave in the axial direction), here the value of n of the basic mode is determined by the geometry of the shell, and is usually larger than unity, except for very short shells.

The practical criterion for the buckling load becomes therefore instead of Eqs. (4.6)

$$\sum_{n=n_b}^{N} C_n S(n,m) =$$

$$\sum_{n=n_b}^{N} C_n \{[(-1)^{m+n} x_2^{2\gamma-2} - 1] G_1(n,m) + K^4 \cos^2\alpha\,[(-1)^{m+n} x_2^{2\gamma} - 1] G_2(n,m)$$

$$+ \eta\,[(-1)^{m+n} x_2^{2\gamma-1} - 1] G_5(n,m) = 0 \qquad \ldots(4.11)$$

where $n_b$ is the number of half waves in the axial direction of the basic mode. The correct value of $n_b$ is that which yields the minimum $\eta$ in the one term solution of Eq. (4.11). An $(N-n_b+1)$ term solution then yields, as before, $(N-n_b+1)$ linear equations, and the buckling load is found from the

$(N - n_b + 1)$ th order determinant of the coefficients of $c_n$. It should be remembered, that as in the case of external pressure, the integral value of t (the number of circumferential waves) which yields the minimum buckling load must be used in the calculations.

The critical load was calculated for a typical shell, Shell (a) of Fig. 2, by 1, 2, 3 and 4 term solutions and compared with the approximate axisymmetric solution of Eq. (4.1). The results are tabulated in Table 9.

## T A B L E 9

### CRITICAL LOAD FOR TYPICAL CONICAL SHELL UNDER UNIFORM AXIAL COMPRESSION

Material : Steel $E = 30 \times 10^6$ psi, $\nu = 0.3$

| Typical Shell | $\alpha^\circ$ | $x_2$ | Taper Ratio | $\rho_{av}/h$ | $(P_{cr}/E) \times 10^3$ | | | | $(P_{cr}/E)$ Axisymmetric |
|---|---|---|---|---|---|---|---|---|---|
| | | | | | 1 term | 2 term | 3 term | 4 term | |
| (a) | 30° | 1.50 | 0.333 | 831 | 28.76 | 28.53 | 28.33 | 28.25 | 28.52 |

The asymmetrical buckling load is indeed very slightly below the axisymmetric one in this example.

The instability behaviour of thin conical shells, under axial compression, within the bounds of linear theory, is similar to that of cylindrical shells. The disagreement of the predictions of linear theory with experimental results is also similar (see Refs. 19 and 43). Hence the linear analysis has practical value only in cases of combined loading.

## REFERENCES


1) Singer, Josef — Buckling of Conical Shells Under Axisymetrical External Pressure. Journal of Mechanical Engineering Science, Vol. 3, No. 4, p. 330, December 1961.
Also, Technion Research and Development Foundation (Israel) AFOSR TN 60-711, November 1960.

2) Seide, Paul — A Donnell Type Theory for Asymmetrical Bending and Buckling of Thin Conical Shells. Journal of Applied Mechanics, Vol. 24, No. 4, p. 547, December, 1957.

3) Seide, Paul — Note on "Stability Equations for Conical Shells". Journal of the Aeronautical Sciences, Vol. 28, No. 5, p. 342, May 1958.

4) Singer, Josef — The Effect of Axial Constraint of the Instability of Thin Circular Cylindrical Shells under External Pressure. Journal of Applied Mechanics, Vol. 27, No. 4, p. 737, December 1960.
Also, Technion Research and Development Foundation (Israel), Technical Note No. 1, Contract No. AF 61 (052)-123, September 1959.

5) Singer, Josef — The Effect of Axial Constraint on the Instability of Thin Conical Shells Under External Pressure. Journal of Applied Mechanics, Vol. 29, No. 1, p. 212, March 1962.

6) Donnell, L.M. — Stability of Thin-Walled Tubes Under Torsion, NACA Report No. 479, 1933.

7) Batdorf, S.R. — A Simplified Method of Elastic Stability Analysis for Thin Cylindrical Shells, NACA Report 874, 1947.

8) Leggett, D.M.A. — The Initial Buckling of Slightly Curved Panels under Combined Shear and Compression. R & M 1972 British A.R.C., 1943.

9) Pflüger, A. — Zur Stabilität der dünnen Kegelschale. Ingenieur-Archiv, Band XIII, Heft. 2, p. 59, 1942.

10) Seide, Paul — On the Buckling of Truncated Conical Shells in Torsion. Journal of Applied Mechanics, Vol. 29, No. 2, p. 321, June 1962.

11) Batdorf, S.B., Stein Manuel, and Schildcrout Murry — Critical Stress of Thin Walled Cylinders in Torsion. NACA TN 1344, June 1947.

12) Flügge, W. — Stresses in Shells, Springer-Verlag, 1960, p. 439.

13) Crate, H., Batdorf, S.B. and Baab, G.W. — The Effect of Internal Pressure on the Buckling Stress of Thin Walled Circular Cylinders Under Torsion. NACA ARR No. 14 E 27, May 1944.

14) Hopkins, H.G., and Brown, E.H. — The Effect of Internal Pressure on the Initial Buckling of Thin-Walled Circular Cylinders Under Torsion. British Aeronautical Research Council, R & M 2423, 1951.

15) Suer, H.S. and Harris, L.A. — The Stability of Thin Walled Cylinders Under Combined Torsion and External Lateral or Hydrostatic Pressure. Journal of Applied Mechanics Vol. 26, No. 1, p. 138, March 1959.

16) Singer, Josef — Buckling of Thin Circular Conical Shells Subjected to Axisymmetrical Temperature Distributions and External Pressure. Technion Research and Development Foundation (Israel), Contract AF 61 (052) – 339, TN, No. 3, July 1961.

17) Singer, J. and Eckstein, A. Experimental Investigations of the Instability of Conical Shells Under External Pressure. Proceedings of the Fourth Annual Conference on Aviation and Astronautics, February 1962, Bulletin of the Research Council of Israel, Vol. 11C, No. 1, April 1962, p. 97.

18) Seide, Paul On the Buckling of Truncated Conical Shells Under Uniform Hydrostatic Pressure. Proceedings of the IUTAM Symposium of the Theory of Thin Elastic Shells, held at Delft, Holland, August 1959, North-Holland Publishing Company, Amsterdam, p. 363.

19) Weingarten, V.I., Morgan, E.J. and Seide, Paul Final Report on the Development of Design Criteria for Elastic Stability of Thin Shell Structures, Space Technology Laboratories, Los Angeles, TR – 60 – 0000 – 19425, December 1960.

20) Westmoreland, R.T. Test of Model Conical Bulkhead-Test 1098, North American Aviation Inc., Missile Development Division, Report MTL 652, May 1956.

21) Homewood, R.H., Brine, A.C. and Johnson, A.E. Jr. Buckling Instability of Monocoque Shells, AVCO Corporation, Research and Advanced Development Division, RAD-TR-9-59-20. August 1959.

22) Holt, M. A Procedure for Determining the Allowable Out-of-Roundness for Vessels Under External Pressure. Transactions ASME, Vol. 74, p. 1225, 1952.

23) Taneda, M. Effect of Initial Out-of-Roundness on the Failure Pressure of Thin Walled Cylinder Subject to Uniform External Pressure. Bulletin of the Japan Society of Mechanical Engineers, Vol. 4, No. 13, p. 25, 1961.

24) Galletly, G.D. and Bart, R. — Effects of Boundary Conditions and Initial Out-of-Roundness on the Strength of Thin-Walled Cylinders Subject to External Hydrostatic Pressure, Journal of Applied Mechanics, Vol. 23, No. 3, September 1956, p. 351.

25) Baruch, M. and Singer, J. — The Effect of Eccentricity on the General Instability of Stiffened Cylindrical Shells Under Hydrostatic Pressure (to be published).

26) Niordson, F.I.N. — Buckling of Conical Shells Subjected to Uniform External Lateral Pressure. Transaction of the Royal Institute of Technology, Sweden, No. 10, 1947.

27) Hoff, N.J. — Buckling and Stability. Forty-First Wilbur Wright Memorial Lecture. Journal of the Royal Aeronautical Society, Vol. 58, No. 517, January 1954, p. 1.

28) Magula, A.W. — Structural Test-Conical Head Assembly – Test No. 815. North American Aviation, Inc., Missile Development Division, Report MTL 531, July 1954.

29) Harris, L.A., Suer, H.S. and Skene, W.T. — Model Investigations of Unstiffened and Stiffened Circular Shells. Experimental Mechanics, Vol. 1, No. 7, July 1961, p. 1.

30) von Mises, R. — Der kritische Aussendruck für allseits belastete zylindrischer Rohre, Festschrift zum 70. Geburtstag von Prof. Dr. A. Stodola, Zurich, 1929, p. 418.

31) Galletly, G.D. and Reynolds, T.E. — A Simple Extension of Southwell's Method for Determining the Elastic General Instability Pressure of Ring-Stiffened Cylinders Subject to External Hydrostatic Pressure. Proceedings of the Society for Experimental Stress Analysis, Vol. 13, No. 2, 1956, p. 141.

32) Bodner, S.R, and Berks, W. — The Effect of Imperfections on the Stress in a Circular Cylindrical Shell Under Hydrostatic Pressure. Polytechnic Insitute of Brooklyn, PIBAL Report No. 210, 1952.

33) Nash, W.A. — Effect of Large Deflections and Initial Imperfections on the Buckling of Cylindrical Shells Subject to Hydrostatic Pressure. Journal of the Aeronautical Sciences, Vol. 22, No. 4, April 1955, p. 264.

34) Donnell, L.H. — Effect of Imperfections on Buckling of Thin Cylinders Under External Pressure, Journal of Applied Mechanics, Vol. 23, No. 4, December 1956, p. 569.

35) Wenk, E., Slankard, R.C. and Nash, W.A. — Experimental Analysis of the Buckling of Cylindrical Shells Subjected to External Hydrostatic Pressure. Proceedings of the Society for Experimental Stress Analysis, Vol. 12, No. 1, 1954, p. 163.

36) Galletly, G.D., Slankard, R.C. and Wenk, E. — General Instability of Ring-Stiffened Cylindrical Shells Subject to External Hydrostatic Pressure – A Comparison of Theory and Experiment. Journal of Applied Mechanics, Vol. 25, No. 2, June 1958, p. 259.

37) Ebner, H. and Schnell, W. — Einbeulen von Kreiszylinderschalen mit abgestufter Wandstärke unter Aussendruck. Zeitschrift für Flugwissenschaften, Vol. 10, Heft 4/5, April 1961.

38) Lundquist, E.E. and Schuette, E.H. — Strength Tests of Thin-Wall Truncated Cones of Circular Section. NACA WRL – 142, December 1942.

39) Nash, W.A. — An Experimental Analysis of the Buckling of Thin Initially Imperfect Cylindrical Shells Subject to Torsion. Proceedings, Society for Experimental Stress Analysis, Vol. 16, No. 2, 1959, p. 55.

40) Seide, Paul — Axisymmetrical Buckling of Circular Cones Under Axial Compression. Journal of Applied Mechanics, Vol. 23, No. 4, December 1956, p. 625.

41) Seide, Paul — The Stability of Thin Conical Frustrums Subjected to Axial Compression and Internal or External Uniform Hydrostatic Pressure. Space Technology Laboratories Inc., Report AF BMD-TR-61-37, March 1961.

42) Singer, Josef — The Effect of Axial Constraint on the Instability of Thin Circular Cylindrical Shells Under Uniform Axial Compression. International Journal of Mechanical Sciences, Vol. 4, No. 2, 1962, p. 253.

43) Lackman, L. and Penzien, J. — Buckling of Circular Cones Under Axial Compression. Journal of Applied Mechanics, Vol. 27, No. 3, September 1960, p. 458.

## ACKNOWLEDGMENT

*The authors would like to thank the Israel Defence Forces for the use of their Philco 2000 Computer and Dr. A. Betzer of the Department of Mechanics for the preparation of programs, as well as Mrs. R. Ferscht-Scher, Miss J. Tarsky, Messrs. A. Herscovici, Y. Goldrei, G. Alony and S. Rubinstein for their help with the computations and Messrs. A. Klausner, O. Shpak and A. Lavy for their assistance during the course of the tests.*

# A P P E N D I X A

## DEFINITIONS OF FUNCTIONS $G_1$, $G_2$ AND $G_3$

The general expressions of the G function are

$$G_1(n,m) = F_1(n)\left[\frac{m+n}{4(\gamma-1)^2+(m+n)^2\beta^2} + \frac{m-n}{4(\gamma-1)^2+(m-n)^2\beta^2}\right] + F_2(n)\left[\frac{1}{4(\gamma-1)^2+(m+n)^2\beta^2} - \frac{1}{4(\gamma-1)^2+(m-n)^2\beta^2}\right] \quad (A\ 1)$$

$$G_2(n,m) = F_3(n)\left[\frac{m+n}{4\gamma^2+(m+n)^2\beta^2} + \frac{m-n}{4\gamma^2+(m-n)^2\beta^2}\right] + F_4(n)\left[\frac{1}{4\gamma^2+(m+n)^2\beta^2} - \frac{1}{4\gamma^2+(m-n)^2\beta^2}\right] \quad (A\ 2)$$

$$G_3(n,m) = F_5(n)\left[\frac{m+n}{(2\gamma+1)^2+(m+n)^2\beta^2} + \frac{m-n}{(2\gamma+1)^2+(m-n)^2\beta^2}\right] + F_6(n)\left[\frac{1}{(2\gamma+1)^2+(m+n)^2\beta^2} - \frac{1}{(2\gamma+1)^2+(m-n)^2\beta^2}\right] \quad (A\ 3)$$

where

$$F_1(n) = 4n\beta^2\{[(\gamma^3-3\gamma^2+2\gamma)-n^2\beta^2(\gamma-1)]-(t^2/\sin^2\alpha)(\gamma-1)\} \quad (A\ 4)$$

$$F_2(n) = 2(\gamma-1)\{[(\gamma^4-4\gamma^3+4\gamma^2)-n^2\beta^2(6\gamma^2-12\gamma+4)+n^4\beta^4] - 2(t^2/\sin^2\alpha)[(\gamma^2-2\gamma+2)-n^2\beta^2]+(t^4/\sin^4\alpha)\} \quad (A\ 5)$$

$$F_3(n) = [2\gamma n\beta^2/(U^2+V^2)]\{\sin^2\alpha[(-\gamma^4+2\gamma^2-1)-n^2\beta^2 2(\gamma^2+1)+n^4\beta^4(-1)] - 2t^2[(\gamma^4+2\gamma^2-1)-n^2\beta^2 2(-\gamma^2+1)+n^4\beta^4] + t^4/\sin^2\alpha)[(2\gamma^2-1)-n^2\beta^2(2)]\} \quad (A\ 6)$$

$$U^2 + V^2 = \sin^4 \alpha [(\gamma^2 - 1)^4 - n^2 \beta^2 4 (-\gamma^6 + \gamma^4 + \gamma^2 - 1) + n^4 \beta^4 (6\gamma^4 + 4\gamma^2 + 6)$$

$$- n^6 \beta^6 4 (-\gamma^2 - 1) + n^8 \beta^8]$$

$$-4t^2 \sin^2 \alpha [(\gamma^6 - \gamma^4 - \gamma^2 + 1) - n^2 \beta^2 (-\gamma^4 + 10\gamma^2 - 1) + n^4 \beta^4 (-\gamma^2 - 1) - n^6 \beta^6]$$

$$+ t^4 [(6\gamma^4 + 4\gamma^2 + 6) - n^2 \beta^2 4(\gamma^2 + 1) + n^4 \beta^4 (6)]$$

$$-4(t^6/\sin^2 \alpha) [(\gamma^2 + 1) - n^2 \beta^2]$$

$$+ (t^8/\sin^4 \alpha) \qquad \text{(A 7)}$$

$$F_4 (n) = [2\gamma/(U^2 + V^2)] \{ \sin^2 \alpha [(\gamma^8 - 3\gamma^6 + 3\gamma^4 - \gamma^2) - n^2 \beta^2 (-4\gamma^6 + 3\gamma^4 + 2\gamma^2 - 1)$$

$$+ n^4 \beta^4 (6\gamma^4 + 3\gamma^2 + 3) - n^6 \beta^6 (-4\gamma^2 - 3) + n^8 \beta^8]$$

$$- 2t^2 [(\gamma^6 - \gamma^2) - n^2 \beta^2 (-\gamma^4 + 8\gamma^2 - 1) + n^4 \beta^4 (-\gamma^2) - n^6 \beta^6]$$

$$+ (t^4/\sin^2 \alpha) [(\gamma^4 - \gamma^2) - n^2 \beta^2 (6\gamma^2 - 1) + n^4 \beta^4] \} \qquad \text{(A 8)}$$

$$F_5 (n) = n \beta^2 [(2\gamma + 1)/2] \qquad \text{(A 9)}$$

and

$$F_6 (n) = [(2\gamma + 1)/2] \{ [(\gamma^2 + \gamma) - n^2 \beta^2] - 2 (t^2/\sin^2 \alpha) \} \qquad \text{(A 10)}$$

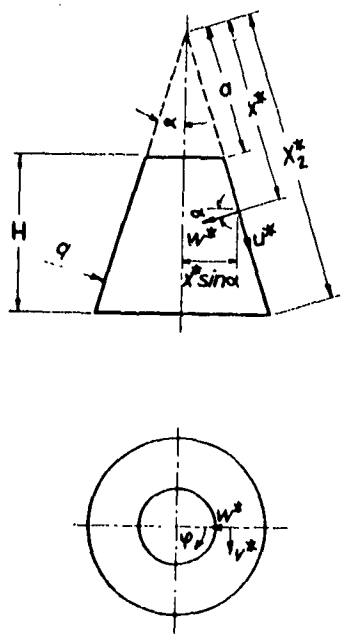


FIG. 1 NOTATION

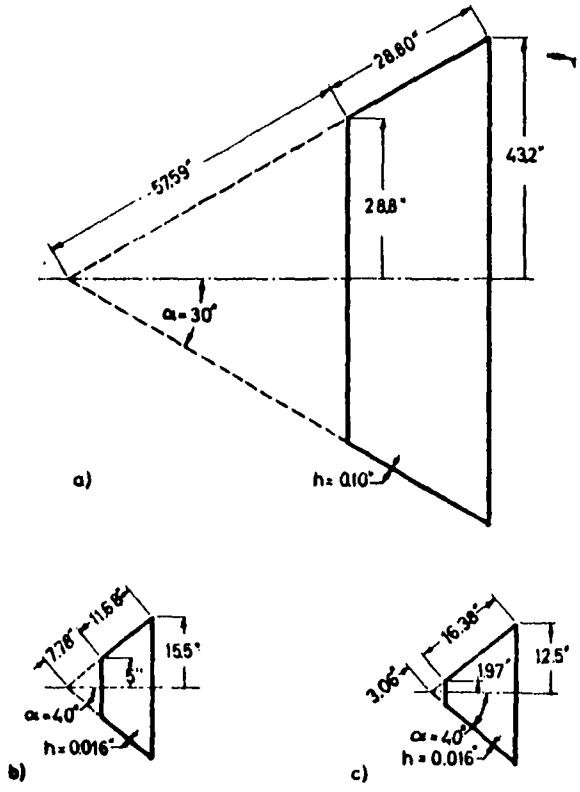


FIG. 2 DIMENSIONS OF TYPICAL CONICAL SHELLS

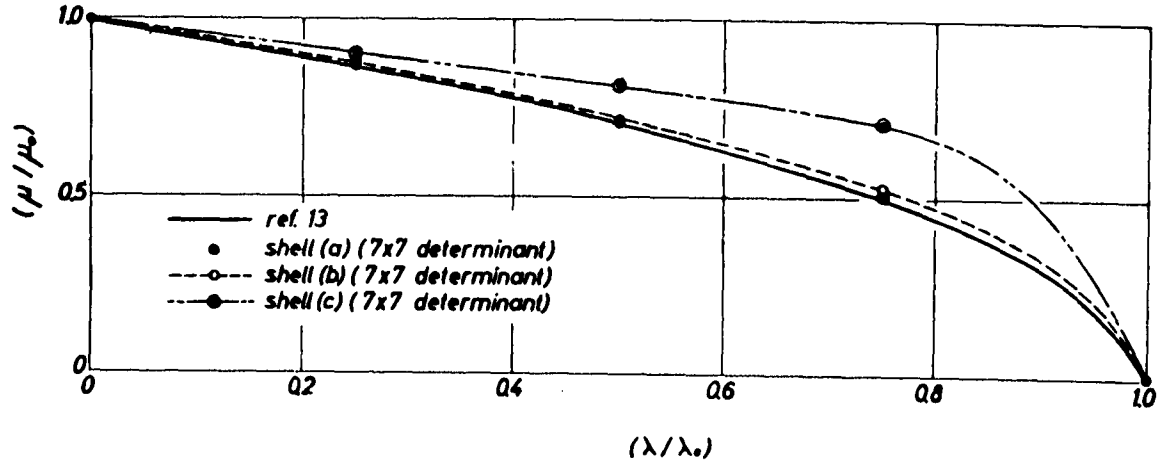


FIG. 3 INTERACTION CURVES FOR TRUNCATED CONICAL SHELLS UNDER COMBINED TORSION AND EXTERNAL HYDROSTATIC PRESSURE

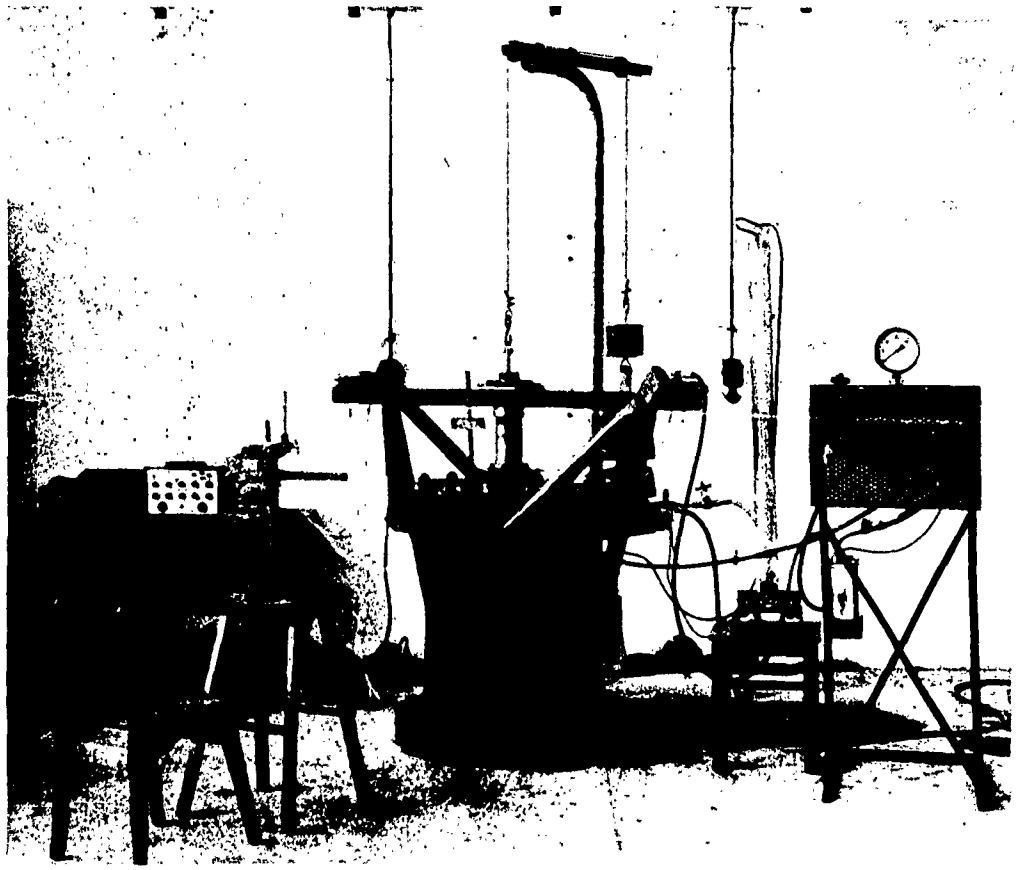

Fig. 4. Test Setup for Combined Torsion and External Pressure Loading.

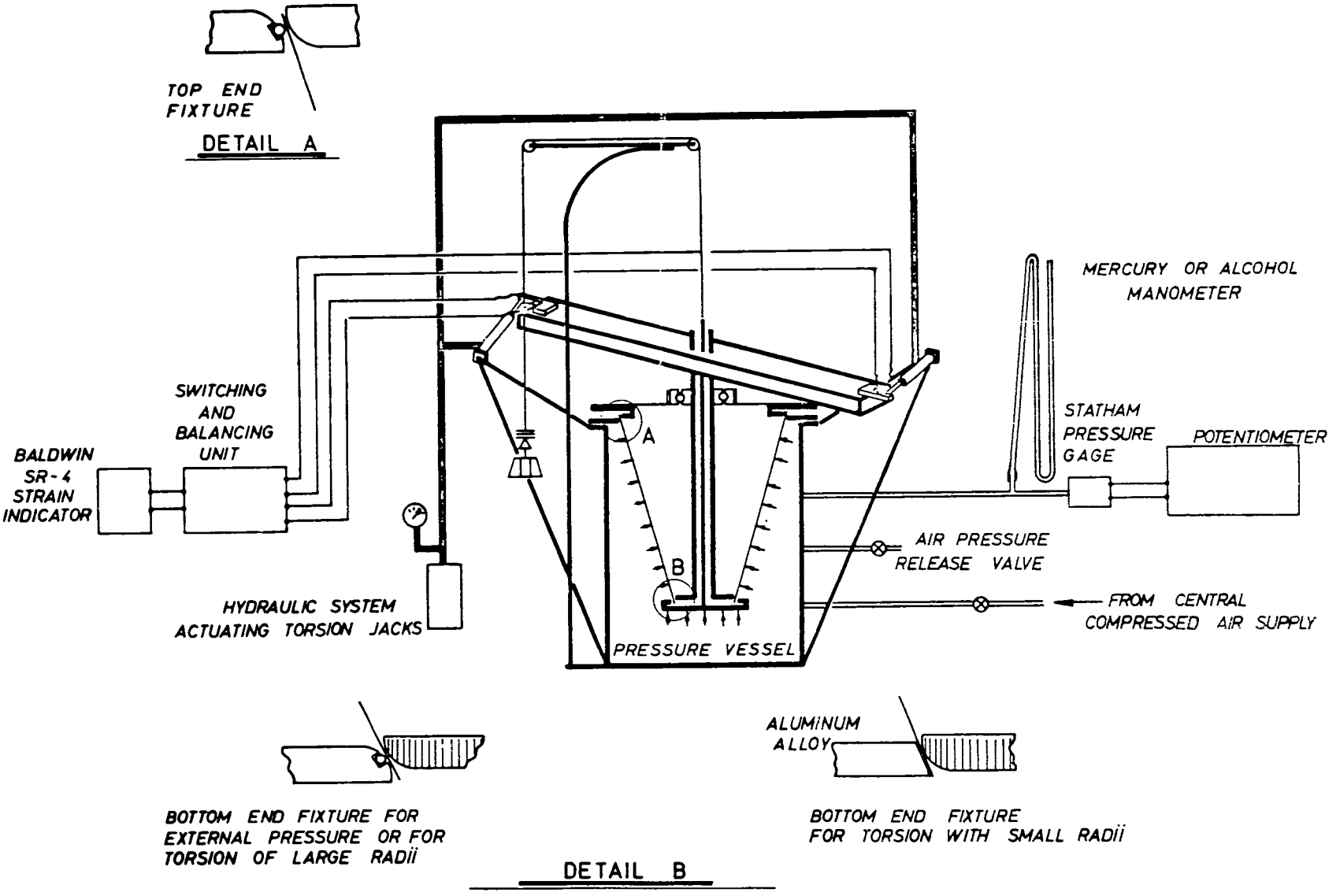


**FIG. 5 TEST SETUP - SCHEMATIC**

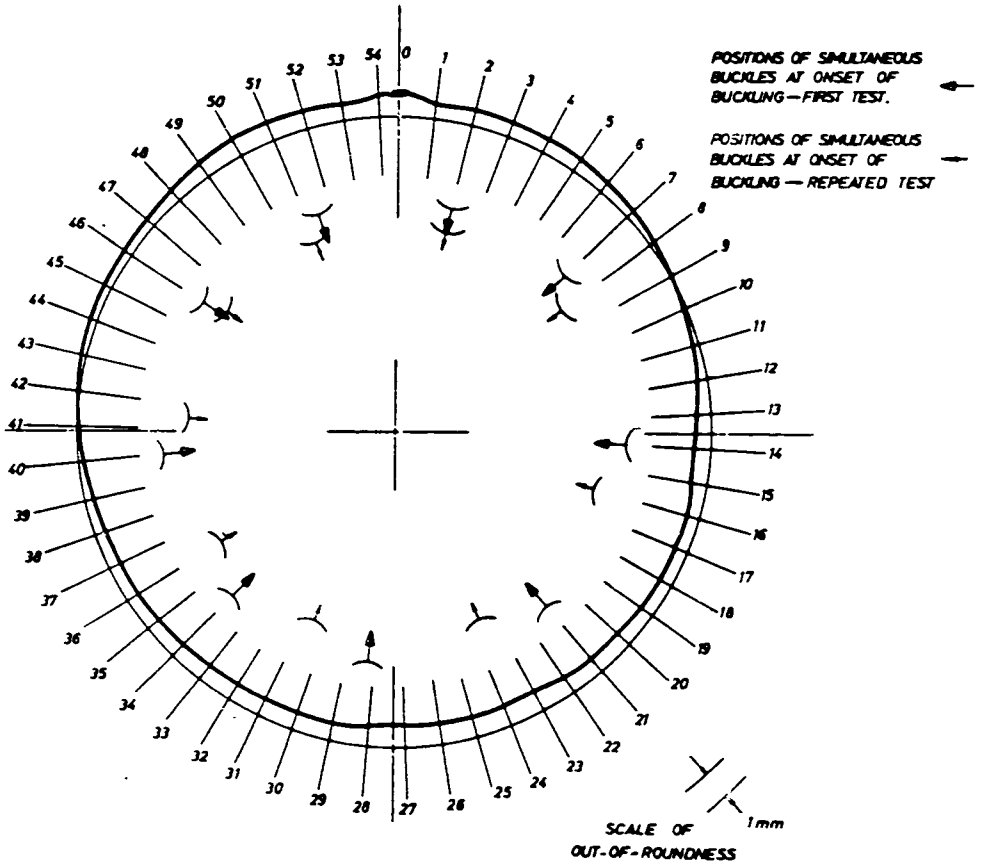


FIG. 7 TYPICAL INITIAL CIRCULARITY CONTOUR

(The out-of-roundness is magnified 20 times)

SPECIMEN 421/5

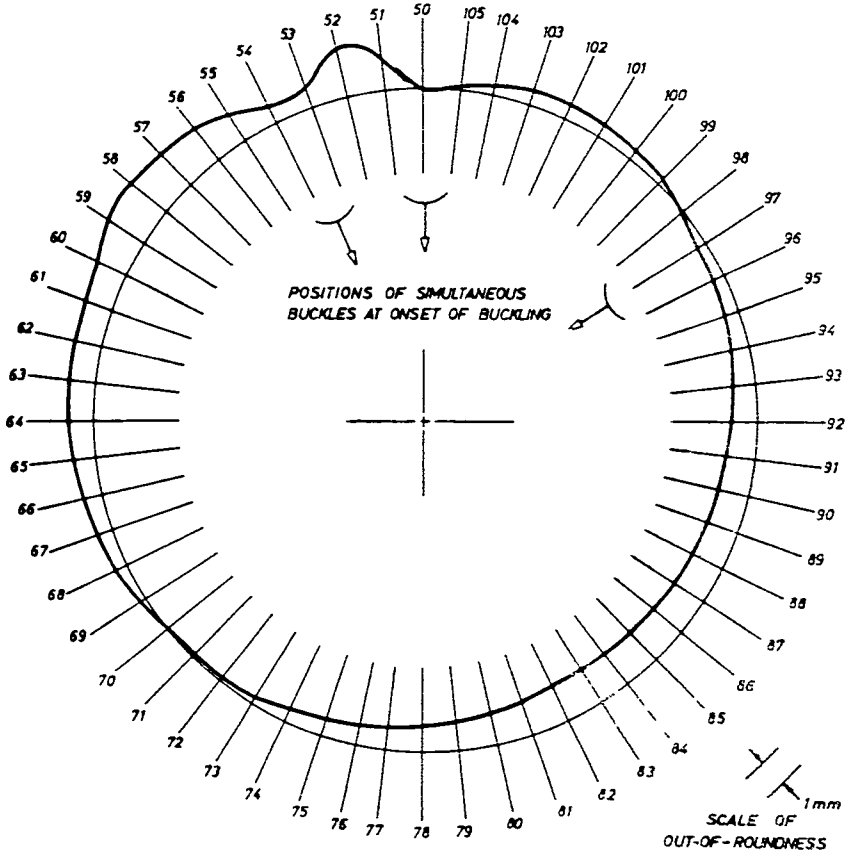


FIG. 8 TYPICAL INITIAL CIRCULARITY CONTOUR

(The out-of-roundness is magnified 20 times)

SPECIMEN 321/4

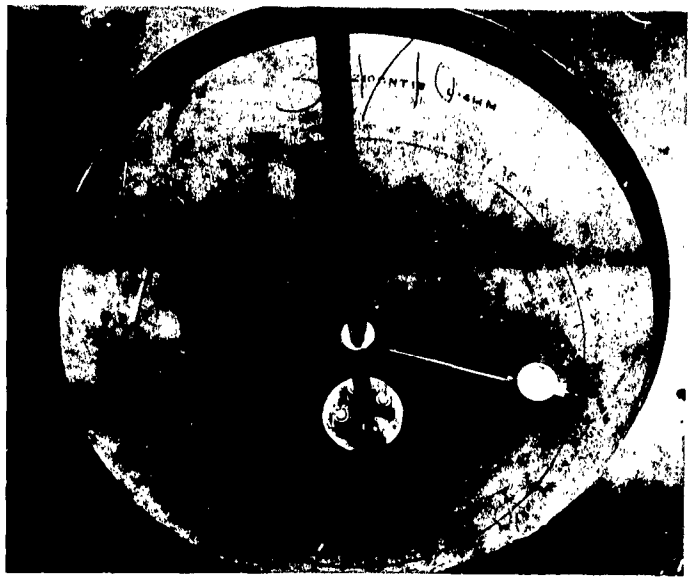

Fig. 6. Device for Measurement of Out-of-Roundness.

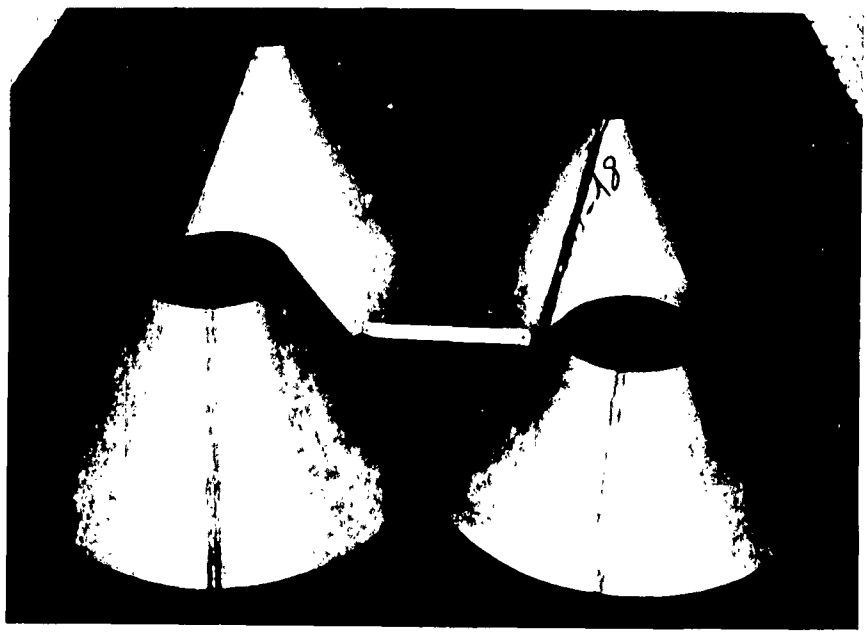

Fig. 9. Typical Specimens – Stee

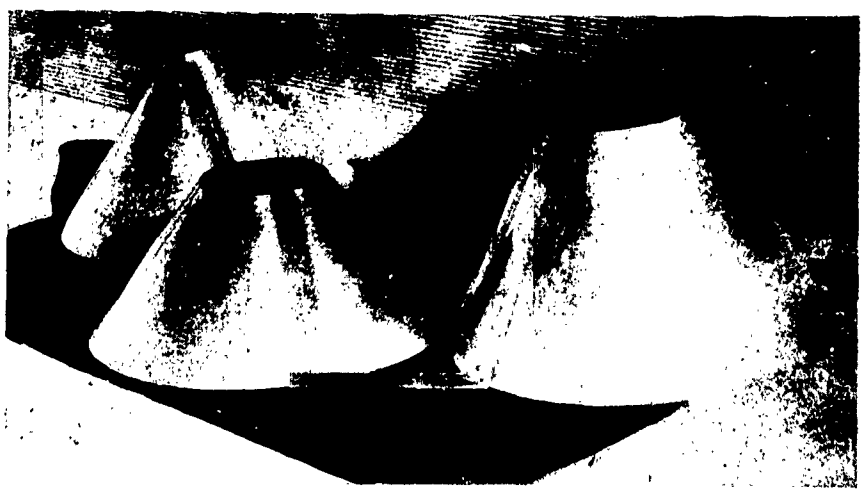

Fig. 10. Typical Specimens – Alcl

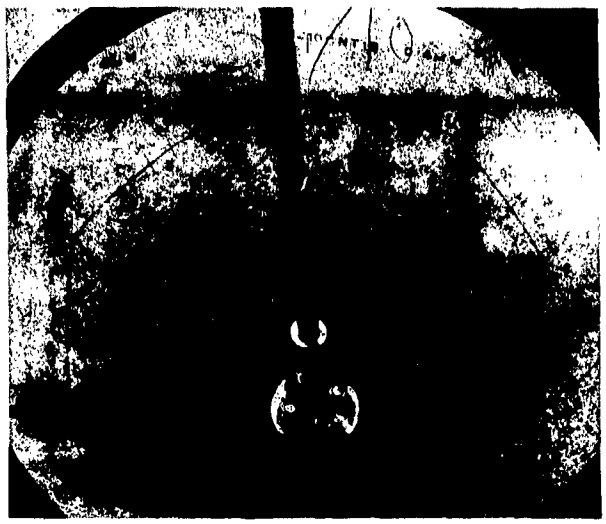

Fig. 11. Typical Buckle Pattern in Fully Buckled State, Resulting from External Pressure Loading (seen from above) – Steel Specimen 311/10.

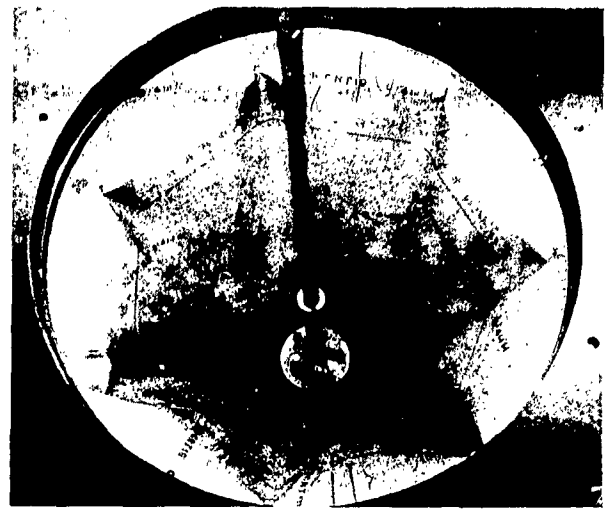

Fig. 12. Typical Buckle Pattern at Plastic Collapse, Resulting from External Pressure Loading. Same Shell as in Fig. 11 – 311/10.

Fig. 13. Typical Buckle Pattern in Fully Buckled State, Resulting from External Pressure Loading (seen from above) – Alclad Specimen 421/5.

Fig. 14. Typical Buckle Pattern at Plastic Collapse, Resulting from External Pressure Loading (seen from above). Same Shell as in Fig. 13 – 421/5.

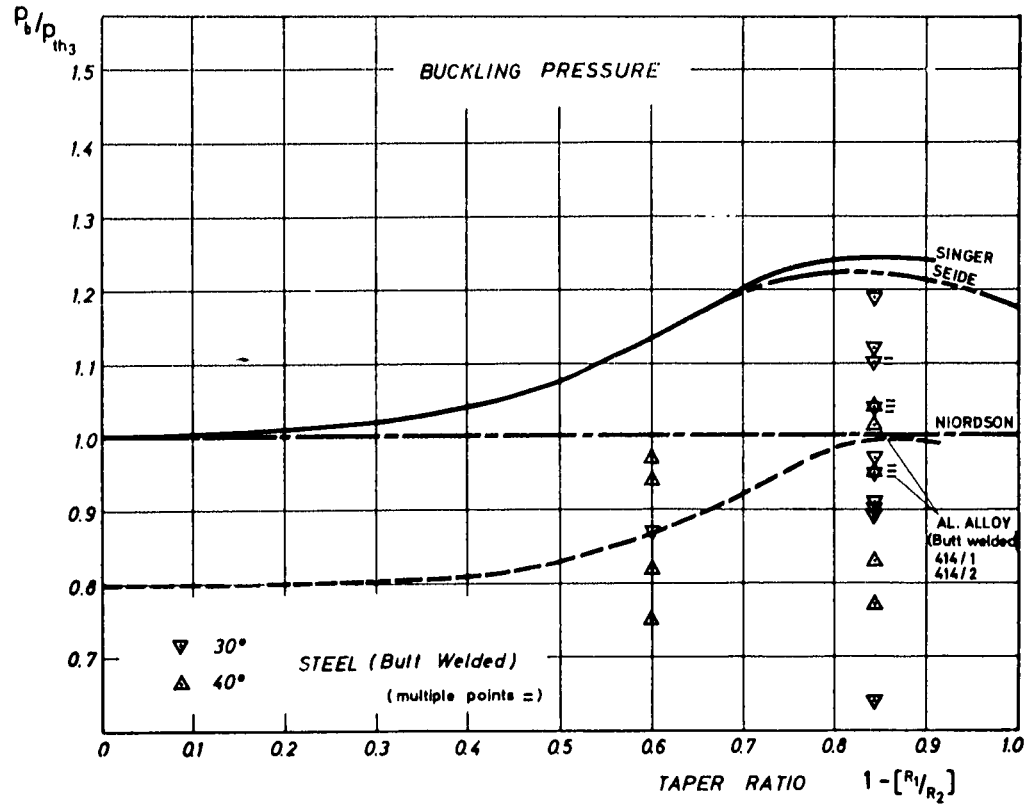


FIG. 15 RATIO OF BUCKLING PRESSURE $p_b$ TO THAT PREDICTED FOR EQUIVALENT CYLINDRICAL SHELL (Niordson) $p_{th_3}$ FOR BUTT-WELDED STEEL CONES (and two aluminum alloys cones).

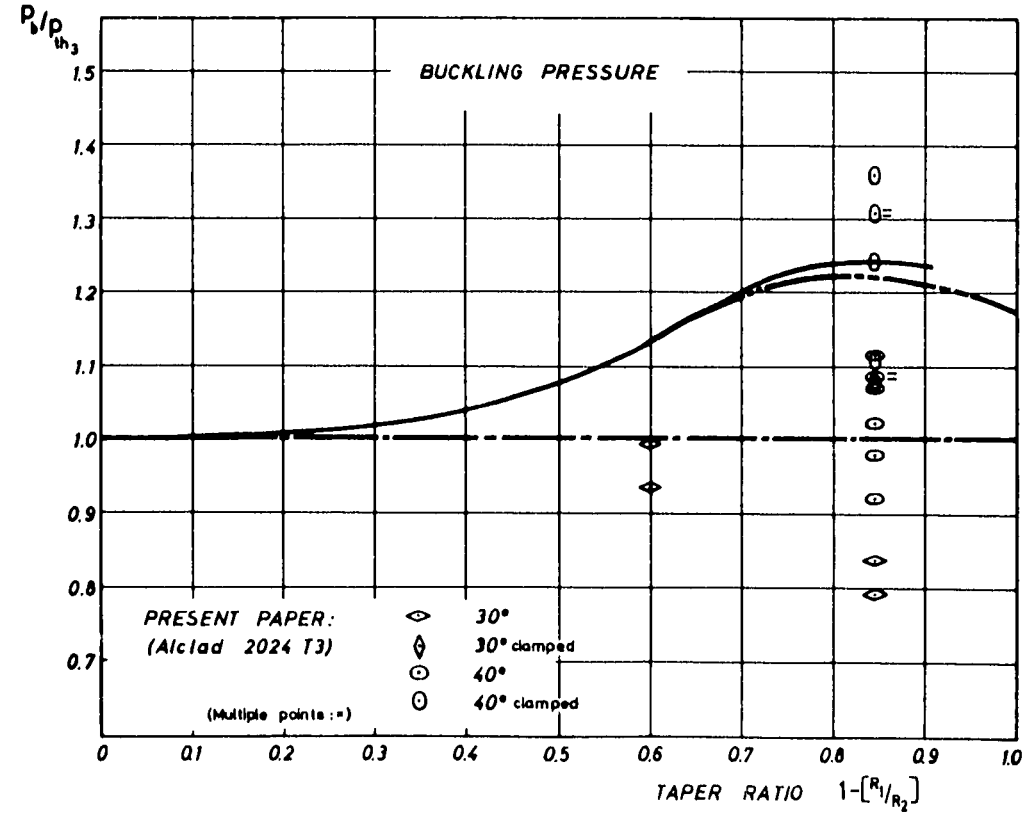


FIG. 16 RATIO OF BUCKLING PRESSURE $p_b$ TO THAT PREDICTED FOR EQUIVALENT CYLINDRICAL SHELL (Niordson) $p_{th_3}$, FOR ADHESIVE BONDED ALCLAD CONES

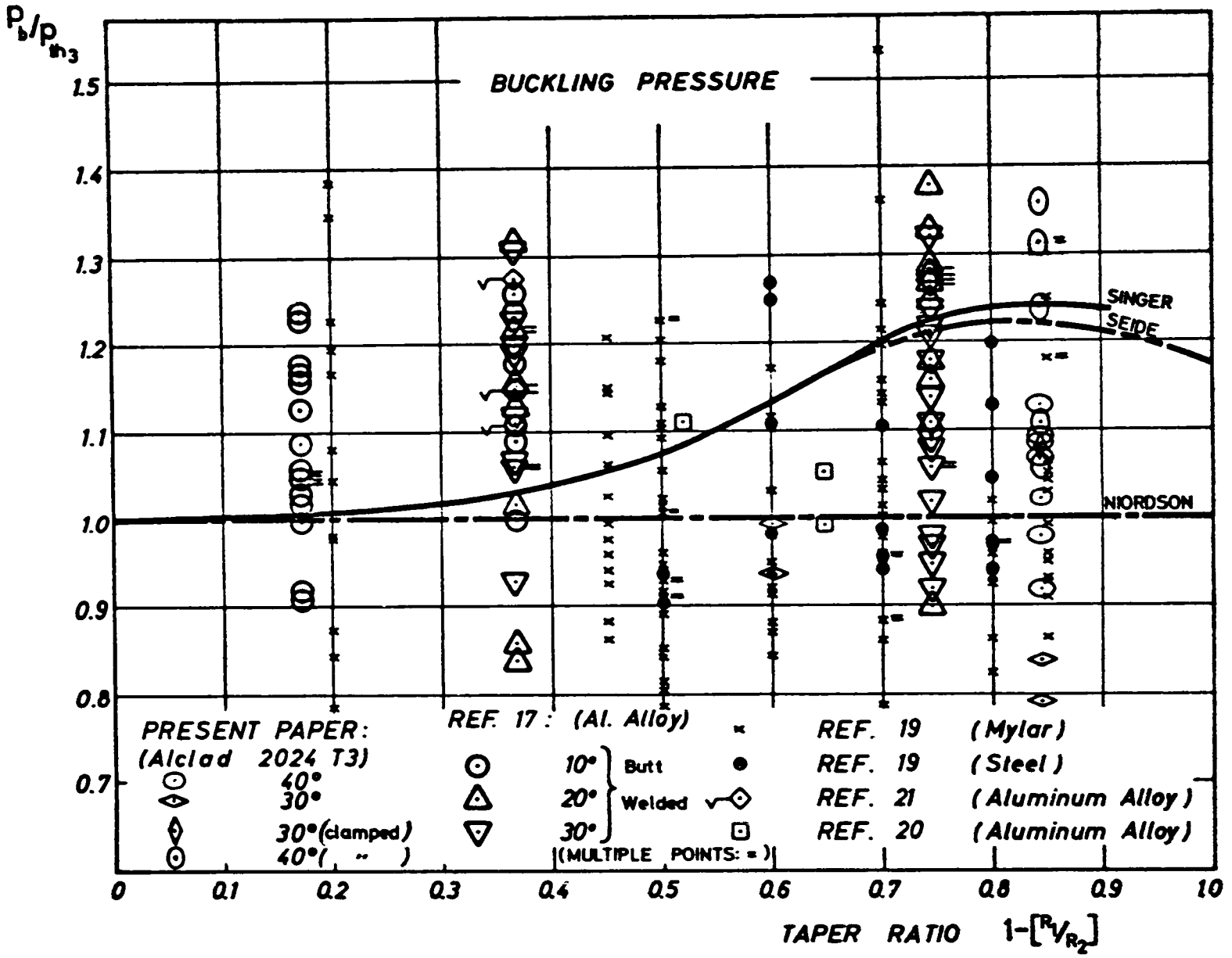


FIG. 17 RATIO OF BUCKLING PRESSURE $p_b$ TO THAT PREDICTED FOR EQUIVALENT CYLINDICAL SHELL (Niordson) $p_{th_3}$, COMPARISON OF RESULTS WITH OTHER EXPERIMENTAL DATA

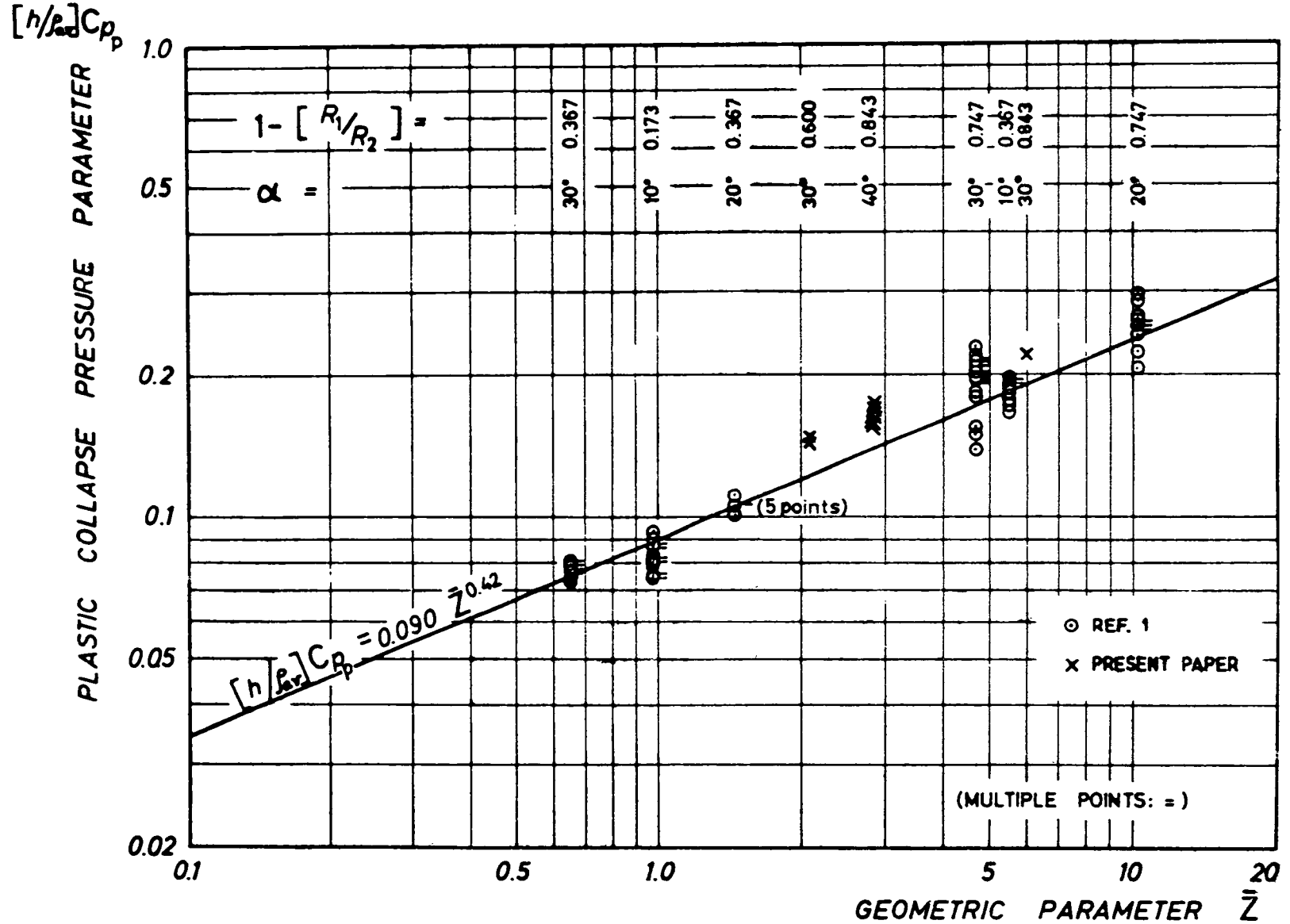


FIG. 18 PLASTIC COLLAPSE PRESSURE COEFFICIENTS

Fig. 19. Typical Buckle Pattern for Conical Shell of Large Taper Ratio in Torsion (Plastic Deformation Remaining After Removal from Test Rig) – Alclad, Specimen 321/6.

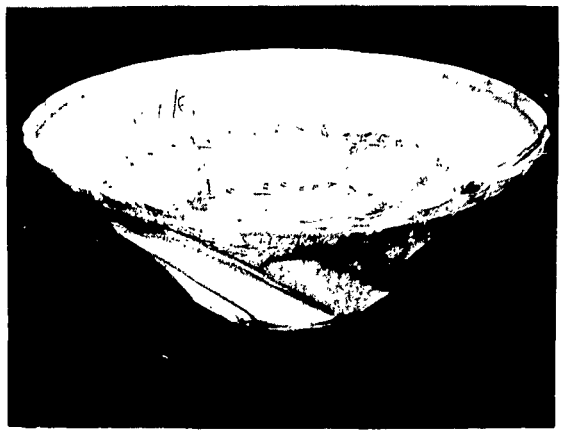

Fig. 20. Typical Buckle Pattern for Conical Shell of Small Taper Ratio (Plastic Deformation Remaining After Removal from Test Rig) – Steel Specimen 417/6.

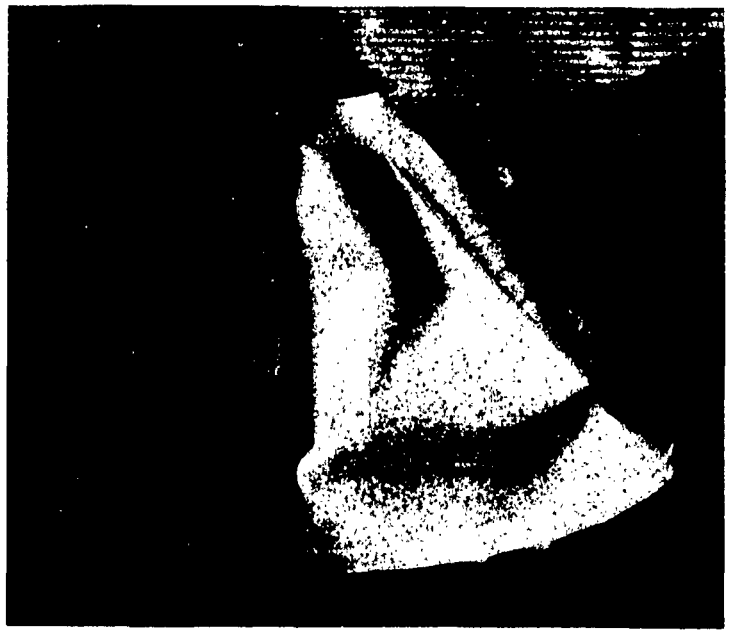

Fig. 23. Typical Buckle Pattern for Conical Shell Under Combined Torsion and External Pressure (Plastic Deformation Remaining After Removal from Test Rig) – Alclad, Specimen 421/9.

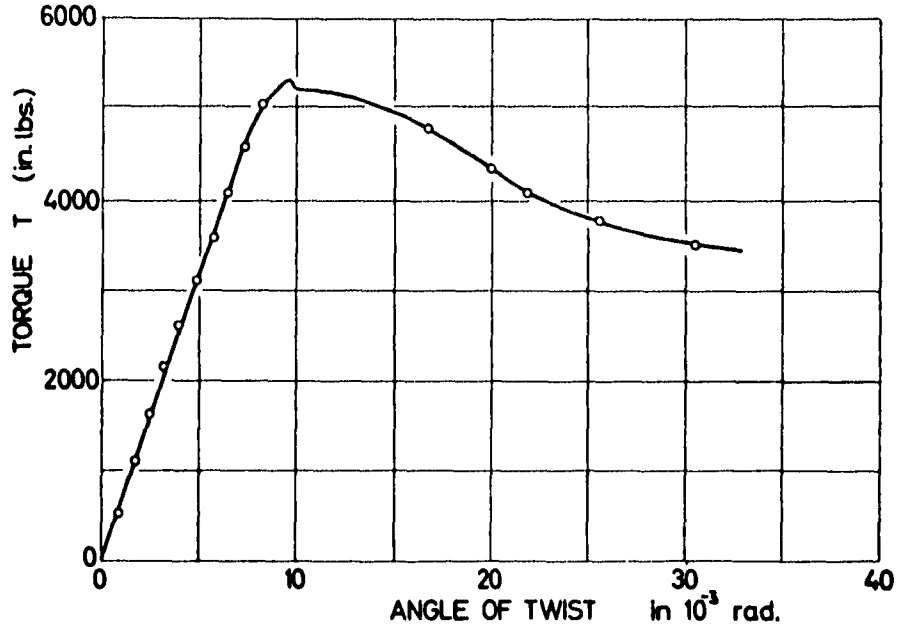


FIG. 21 TYPICAL EXPERIMENTAL CURVE OF TORQUE vs. ANGLE OF TWIST – ALCLAD SPECIMEN 321/6

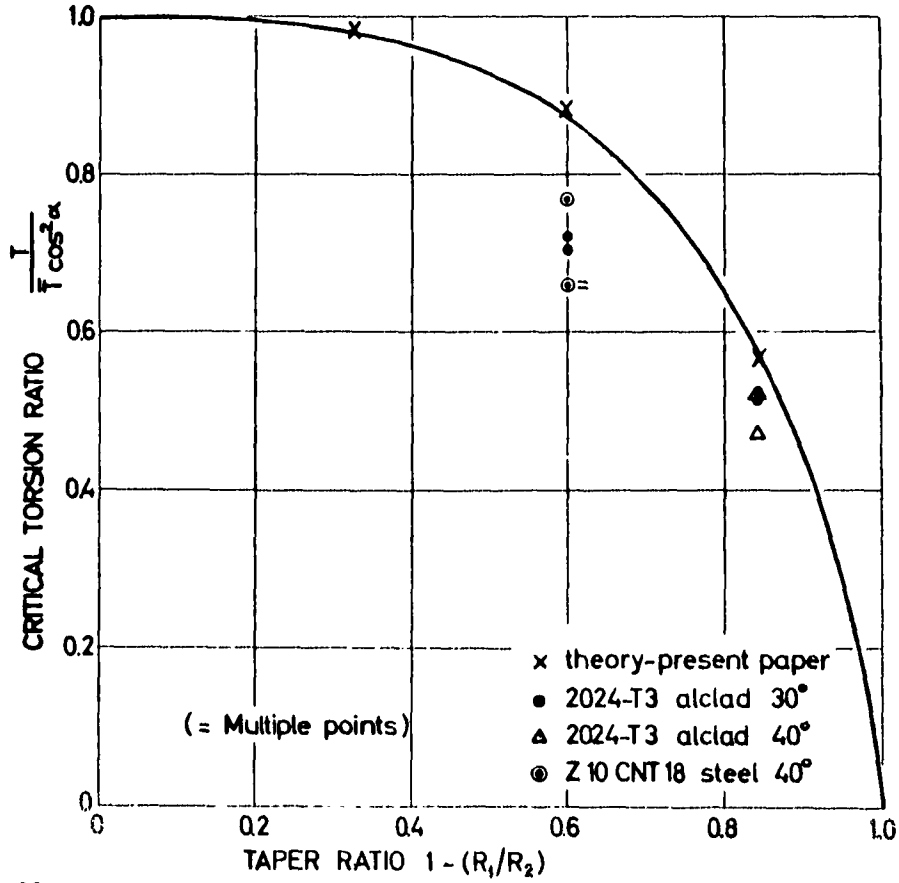


FIG. 22 COMPARISON OF THEORY AND EXPERIMENT FOR BUCKLING OF CONICAL SHELLS IN TORSION

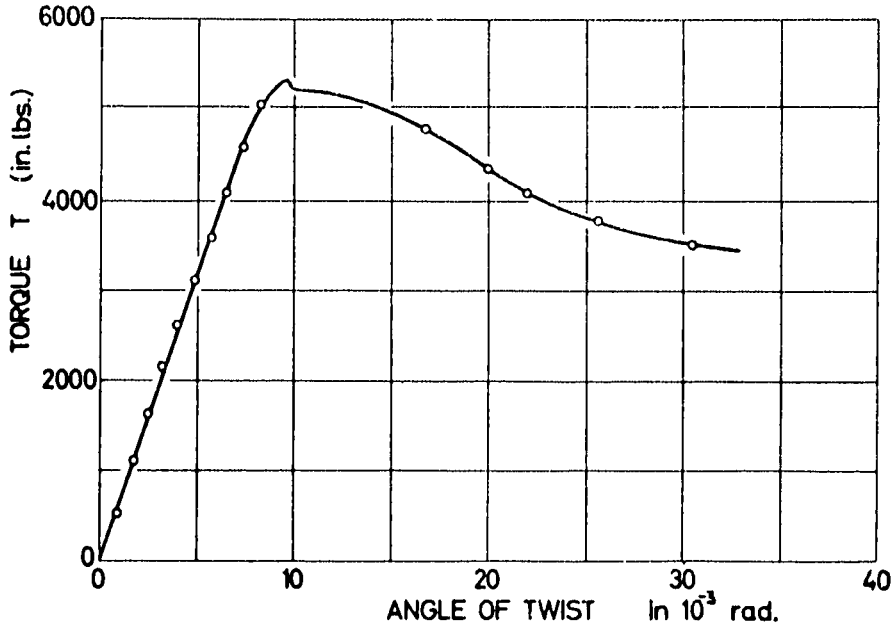


FIG. 21 TYPICAL EXPERIMENTAL CURVE OF TORQUE vs. ANGLE OF TWIST – ALCLAD SPECIMEN 321/6

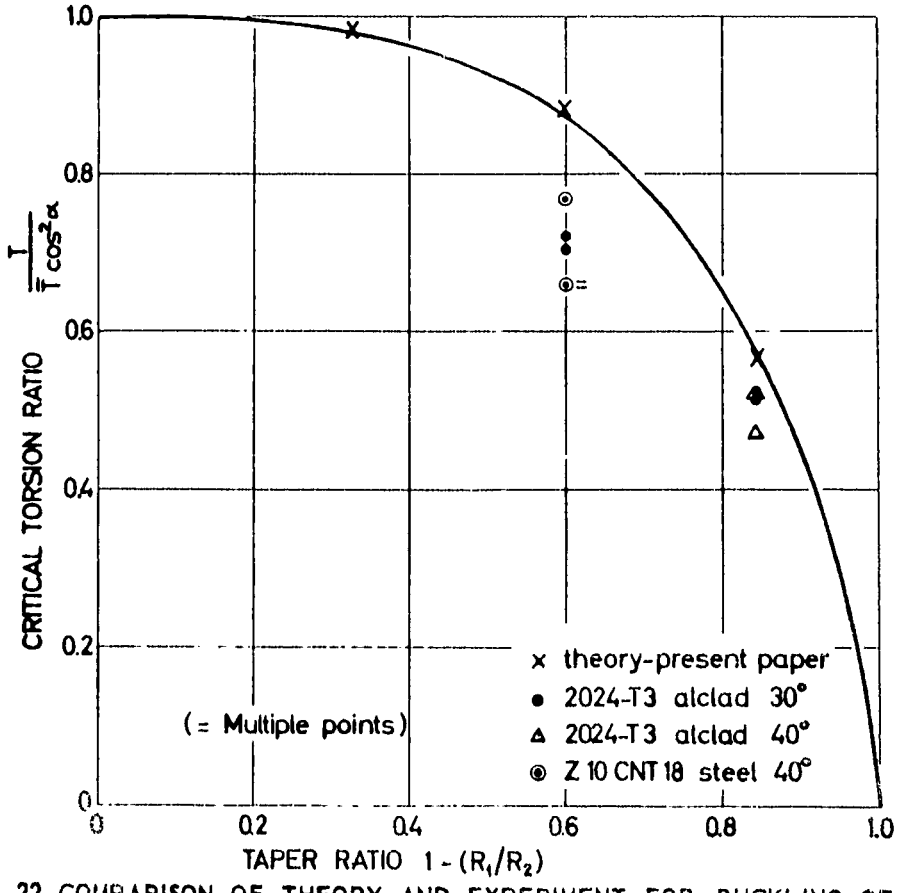


FIG. 22 COMPARISON OF THEORY AND EXPERIMENT FOR BUCKLING OF CONICAL SHELLS IN TORSION

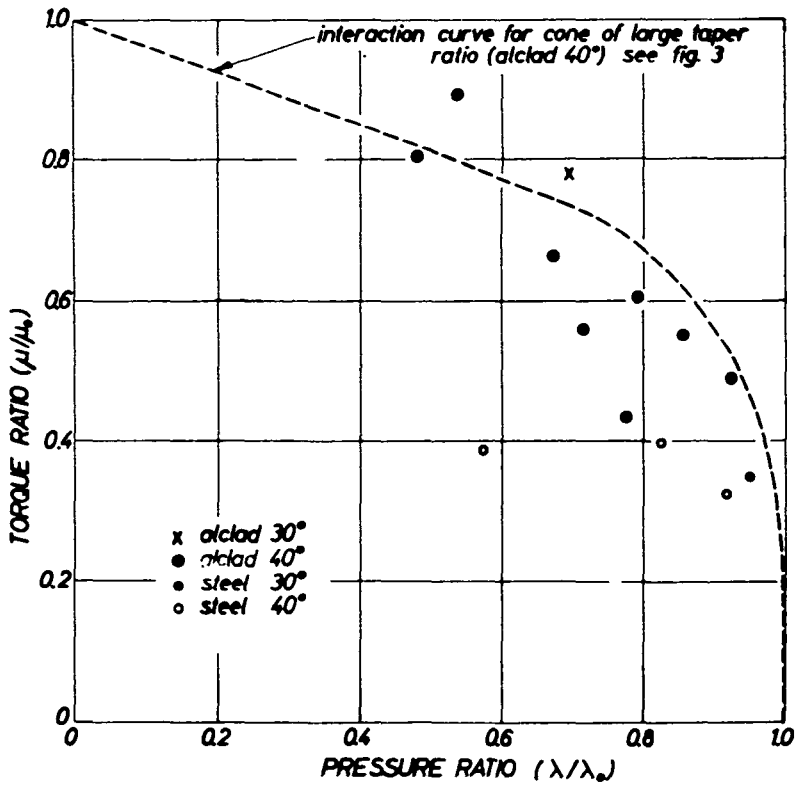


FIG. 24 EXPERIMENTAL VERIFICATION OF INTERACTION CURVE FOR BUCKLING UNDER COMBINED TORSION AND EXTERNAL PRESSURE – SHELLS OF LARGE TAPER RATIO

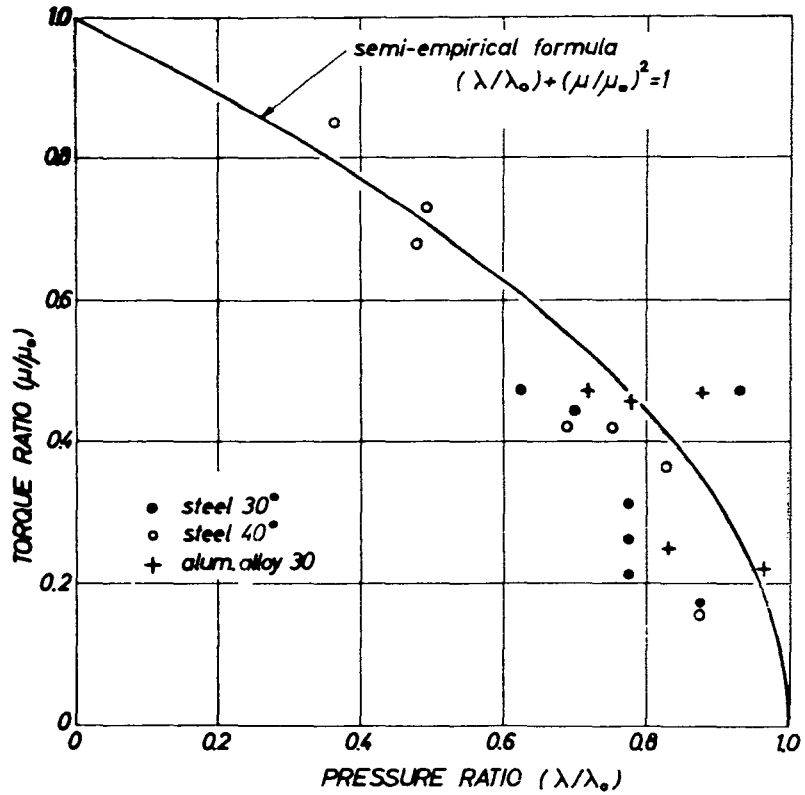


FIG. 25. EXPERIMENTAL VERIFICATION OF INTERACTION CURVE FOR BUCKLING UNDER COMBINED TORSION AND EXTERNAL PRESSURE – SHELLS OF SMALL AND MEDIUM TAPER RATIO

TECHNION RESEARCH & DEVELOPMENT
FOUNDATION, LTD., HAIFA, ISRAEL
TAE REPORT 19
September 1962

AF 61(052)-339
TR
MECHANICS

BUCKLING OF CONICAL SHELLS UNDER EXTERNAL PRESSURE, TORSION AND AXIAL COMPRESSION.

JOSEF SINGER, ABRAHAM ECKSTEIN AND MENAHEM BARUCH.

ABSTRACT: A method developed previously for the analysis of the instability of thin conical shells under external pressure is now extended to buckling under torsion and combined torsion and external or internal pressure as well as axisymmetric temperature distributions. The method is based on solution of modified Donnell type stability equations, in the presence of slightly relaxed boundary conditions for the u and v displacements. Two formulations of the solution for torsion and combined loadings are given and compared. Typical examples are calculated and compared with results obtained by Seide, and interaction curves for combined torsion and external pressure loading are given. For

TECHNION RESEARCH & DEVELOPMENT
FOUNDATION,LTD., HAIFA, ISRAEL
TAE REPORT 19
September 1962

AF 61(052)-339
TR
MECHANICS

BUCKLING OF CONICAL SHELLS UNDER ESTERNAL PRESSURE, TORSION AND AXIAL COMPRESSION.

JOSEF SINGER, ABRAHAM ECKSTEIN AND MENAHEM BARUCH.

ABSTRACT: A method developed previously for the analysis of the instability of thin conical shells under external pressure is now extended to buckling under torsion and combined torsion and external or internal pressure as well as axisymmetric temperature distributions. The method is based on solution of modified Donnell type stability equations, in the presence of slightly relaxed boundary conditions for the u and v displacements. Two formulations of the solution for torsion and combined loadings are given and compared. Typical examples are calculated and compared with results obtained by Seide, and interaction curves for combined torsion and external pressure loading are given. For

TECHNION RESEARCH & DEVELOPMENT
FOUNDATION, LTD., HAIFA, ISRAEL
TAE REPORT 19
September 1962

AF 61(052)-339
TR
MECHANICS

BUCKLING OF CONICAL SHELLS UNDER EXTERNAL PRESSURE, TORSION AND AXIAL COMPRESSION.

JOSEF SINGER, ABRAHAM ECKSTEIN AND MENAHEM BARUCH.

ABSTRACT: A method developed previously for the analysis of the instability of thin conical shells under external pressure is now extended to buckling under torsion and combined torsion and external or internal pressure as well as axisymmetric temperature distributions. The method is based on solution of modified Donnell type stability equations, in the presence of slightly relaxed boundary conditions for the u and v displacements. Two formulations of the solution for torsion and combined loadings are given and compared. Typical examples are calculated and compared with results obtained by Seide, and interaction curves for combined torsion and external pressure loading are given. For

TECHNION RESEARCH & DEVELOPMENT
FOUNDATION,LTD., HAIFA, ISRAEL
TAE REPORT 19
September 1962

AF 61(052)-339
TR
MECHANICS

BUCKLING OF CONICAL SHELLS UNDER ESTERNAL PRESSURE, TORSION AND AXIAL COMPRESSION.

JOSEF SINGER, ABRAHAM ECKSTEIN AND MENAHEM BARUCH.

ABSTRACT: A method developed previously for the analysis of the instability of thin conical shells under external pressure is now extended to buckling under torsion and combined torsion and external or internal pressure as well as axisymmetric temperature distributions. The method is based on solution of modified Donnell type stability equations, in the presence of slightly relaxed boundary conditions for the u and v displacements. Two formulations of the solution for torsion and combined loadings are given and compared. Typical examples are calculated and compared with results obtained by Seide, and interaction curves for combined torsion and external pressure loading are given. For

conical shells of small and medium taper ratio, the interaction curves may be approximated by the semi-empirical curve of Crate, Batdorf and Baab for cylindrical shells, but for large taper ratio different curves are obtained.

The results of a continuation of an experimental program on the instability of thin truncated conical shells under uniform external pressure, carried out at the Department of Aeronautical Engineering, are presented and discussed. The tests of 33 steel, Alclad, and aluminum alloy conical shells of varying geometries are described, and the results are compared and correlated with other experimental investigations and with theory. The test results reverify the theories of Singer and Seide. The buckling and postbuckling behaviour and the effect of initial out-of-roundness are discussed.

The results of another experimental program on the instability of thin truncated conical shells in torsion and under the combined loading of external pressure and torsion are given, and compared with the theories of Section 1. Good agreement was obtained between theory and experiments.

The method of analysis of Section 1 is adapted to analyse the asymmetric buckling of thin conical shells under uniform axial compression. A linear theory is used and typical cases are computed and compared with an axisymmetric analysis.

conical shells of small and medium taper ratio, the interaction curves may be approximated by the semi-empirical curve of Crate, Batdorf and Baab for cylindrical shells, but for large taper ratio different curves are obtained.

The results of a continuation of an experimental program on the instability of thin truncated conical shells under uniform external pressure, carried out at the Department of Aeronautical Engineering, are presented and discussed. The tests of 33 steel, Alclad, and aluminum alloy conical shells of varying geometries are described, and the results are compared and correlated with other experimental investigations and with theory. The test results reverify the theories of Singer and Seide. The buckling and postbuckling behaviour and the effect of initial out-of-roundness are discussed.

The results of another experimental program on the instability of thin truncated conical shells in torsion and under the combined loading of external pressure and torsion are given, and compared with the theories of Section 1. Good agreement was obtained between theory and experiments.

The method of analysis of Section 1 is adapted to analyse the asymmetric buckling of thin conical shells under uniform axial compression. A linear theory is used and typical cases are computed and compared with an axisymmetric analysis.

conical shells of small and medium taper ratio, the interaction curves may be approximated by the semi-empirical curve of Crate, Batdorf and Baab for cylindrical shells, but for large taper ratio different curves are obtained.

The results of a continuation of an experimental program on the instability of thin truncated conical shells under uniform external pressure, carried out at the Department of Aeronautical Engineering, are presented and discussed. The tests of 33 steel, Alclad, and aluminum alloy conical shells of varying geometries are described, and the results are compared and correlated with other experimental investigations and with theory. The test results reverify the theories of Singer and Seide. The buckling and postbuckling behaviour and the effect of initial out-of-roundness are discussed.

The results of another experimental program on the instability of thin truncated conical shells in torsion and under the combined loading of external pressure and torsion are given, and compared with the theories of Section 1. Good agreement was obtained between theory and experiments.

The method of analysis of Section 1 is adapted to analyse the asymmetric buckling of thin conical shells under uniform axial compression. A linear theory is used and typical cases are computed and compared with an axisymmetric analysis.